Supplementary Information

Bioinspired Cu(II) complexes with tunable axial donors: Unravelling structure-function correlations in phenoxazinone synthase mimics

Dyuti Bhandary,[§ a] Limashree Sahoo,[§ b] Gunasekaran Velmurugan,[*c] and Gourab Mukherjee*[a,d]

[a.] *Department of Catalysis & Fine Chemicals, CSIR - Indian Institute of Chemical Technology, Hyderabad - 500007, Telangana, India. Email: gmukherj@csiriict.in*

[b.] *Department of Chemistry, Indian Institute of Technology Guwahati, Guwahati - 781039, Assam, India.*

[c.] *Institute of Inorganic Chemistry, Heidelberg University, Im Neuenheimer Feld 270, 69120 Heidelberg, Germany. Email: velmurugan.gunasekaran@aci.uni-heidelberg.de*

[d.] *Academy of Scientific and Innovative Research, Ghaziabad, 201002, India*

[§] Contributed equally.

Synthesis of Ligands:

Scheme S1. General synthetic scheme for the ligands N4, N3O and N3S.

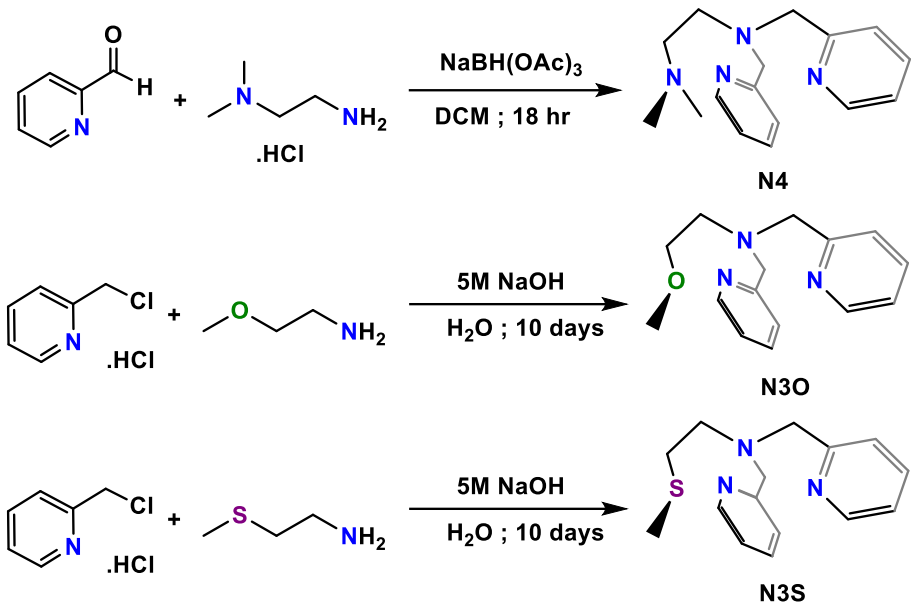

Synthesis of the copper complexes

Scheme S2. General procedure for the synthesis of the Cu(II) complexes.

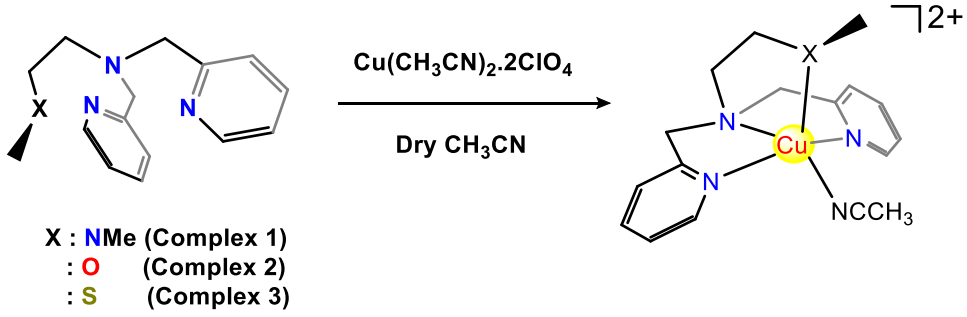

Instrumentation

The copper complexes were characterized by various techniques such as elemental analysis (CHN), UV-Vis spectroscopy, electrospray ionization mass spectrometry (ESI-MS), FT-IR spectroscopy, cyclic voltammetry, electron paramagnetic resonance (EPR) spectroscopy and single crystal X-ray diffraction (XRD) crystallography. The CHN analysis of the copper complexes were carried out in a VarioMICRO superuser setup. UV-Vis spectral data and kinetics experiments were recorded on an Agilent 8453 spectrophotometer and SFA 20 rapid kinetics accessory (Hi-Tech scientific pneumatic drive unit) coupled with a Cary 60 spectrophotometer. ESI-MS data were obtained using the Agilent G6546 series UHPLC-LC/Q-TOF-HRMS mass spectrometer at 298 K with a 2 kV nozzle voltage and 325 °C gas temperature. FT-IR spectroscopy were conducted on the three copper complexes using Bruker Alpha FT-IR spectrophotometer. Cyclic voltammetry spectra (polarographic method) were recorded in dry degassed acetonitrile using CH Instruments electrochemical workstation (CHI 1120B) with a glassy carbon working electrode, a Pt-wire auxiliary, and an Ag/AgCl reference electrode; 0.1 M tetrabutylammonium perchlorate in MeCN was used

as the electrolyte. All the values were reported against Ag/Ag^+ and calibrated with the Fc^+/Fc couple. EPR experiments were done at 77 K in acetonitrile using a JES-FA200 ESR spectrometer, maintaining experimental parameters as follows: frequency at 9138.66 MHz, power at 0.995 mW, field centre at 490.00 mT, width ±500.00 mT, sweep time of 30.0 s, modulation frequency of 100.00 kHz, width at 2 mT, amplitude for CH1=25.0, CH2= 2.0, and a time constant of 0.03 s, consistent across all samples. Single crystal XRD data was collected at room temperature using a single source Super Nova CCD System instrument from Agilent Technologies equipped with a fine focus 1.75 kW sealed tube with MoKα radiation. The data was reduced using CrysAlis RED36. The structural parameters have been reported in one of our recent reports.[1]

Kinetic Experiments

The reactivity studies and reaction kinetic experiments were recorded on a Hewlett-Packard 8453 spectrophotometer equipped with a constant temperature circulating water and/or SFA 20 rapid kinetics accessory (Hi-Tech scientific pneumatic drive unit) coupled with a Cary 60 spectrophotometer. For kinetics, UV-Vis spectral changes were monitored for reactions involving different concentrations of the catalysts or the substrate in the presence of air. The initial rates were obtained by fitting the changes in the absorbance at 420 nm for **1**, **2**, and **3**. The second-order rate constants were evaluated by varying the *o*-Aminophenol (OAP) concentrations and fitting the thus obtained pseudo-first-order rate constants against the concentration of OAP to give a linear fit. Reactions were run in triplicate for reproducibility of the data reported.

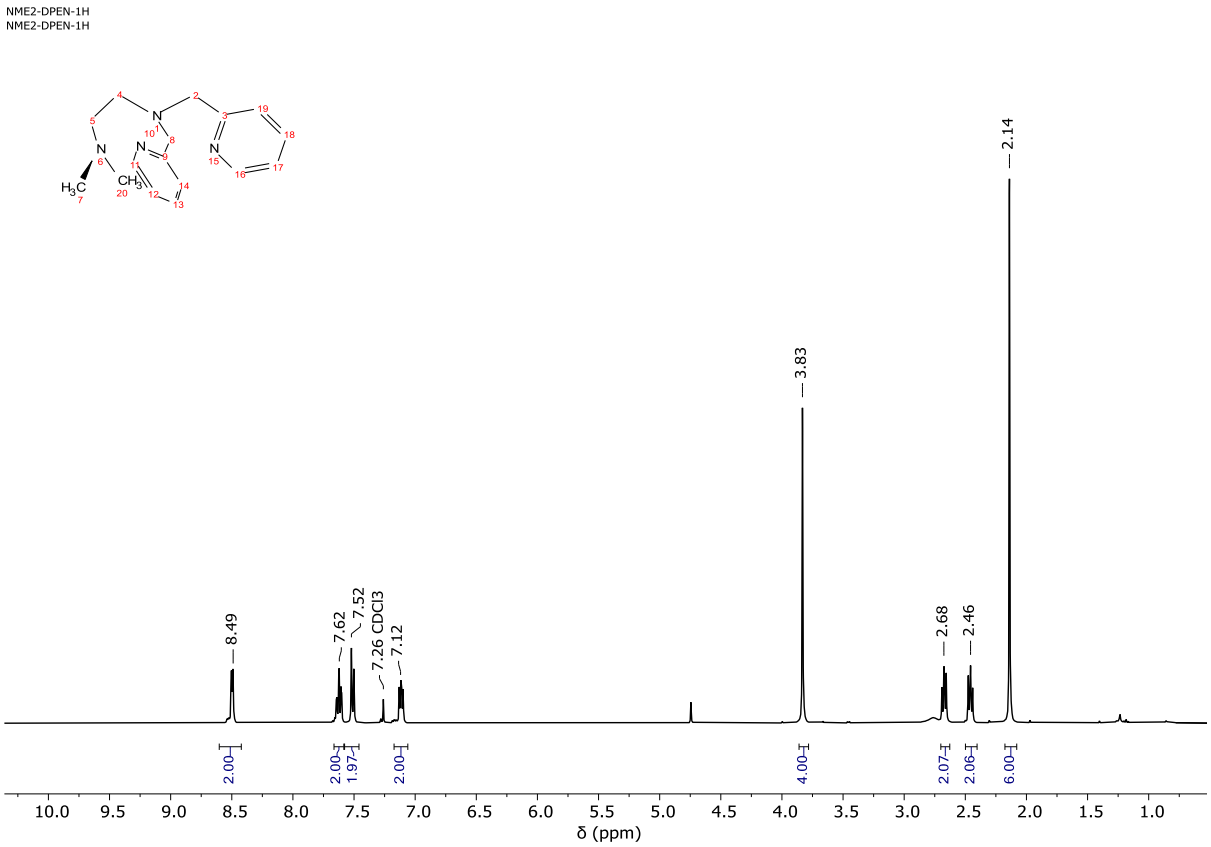

Fig. S1. ^{1}H-NMR (600MHz, $CDCl_3$) spectrum of the ligand N4.

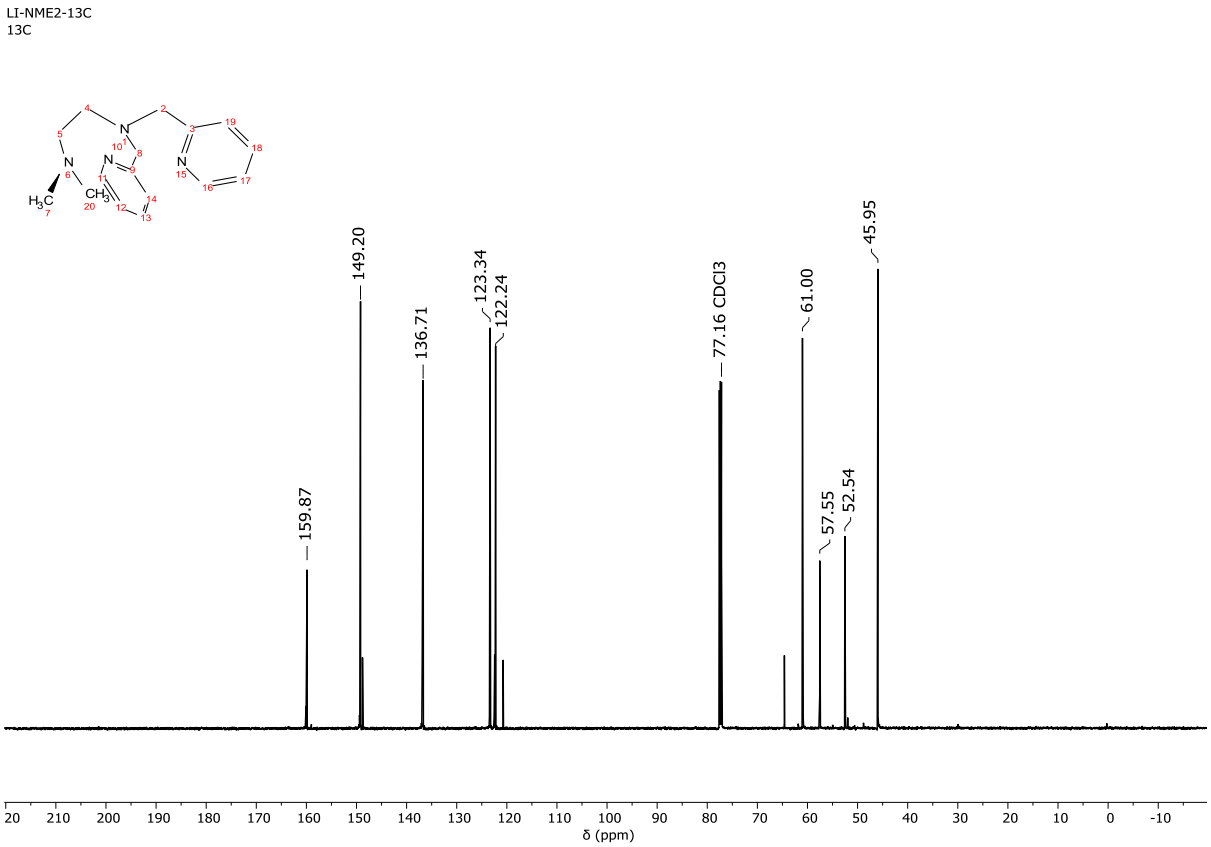

Fig. S2. $^{13}C\{^{1}H\}$ NMR (125MHz, $CDCl_3$) spectrum of the ligand N4.

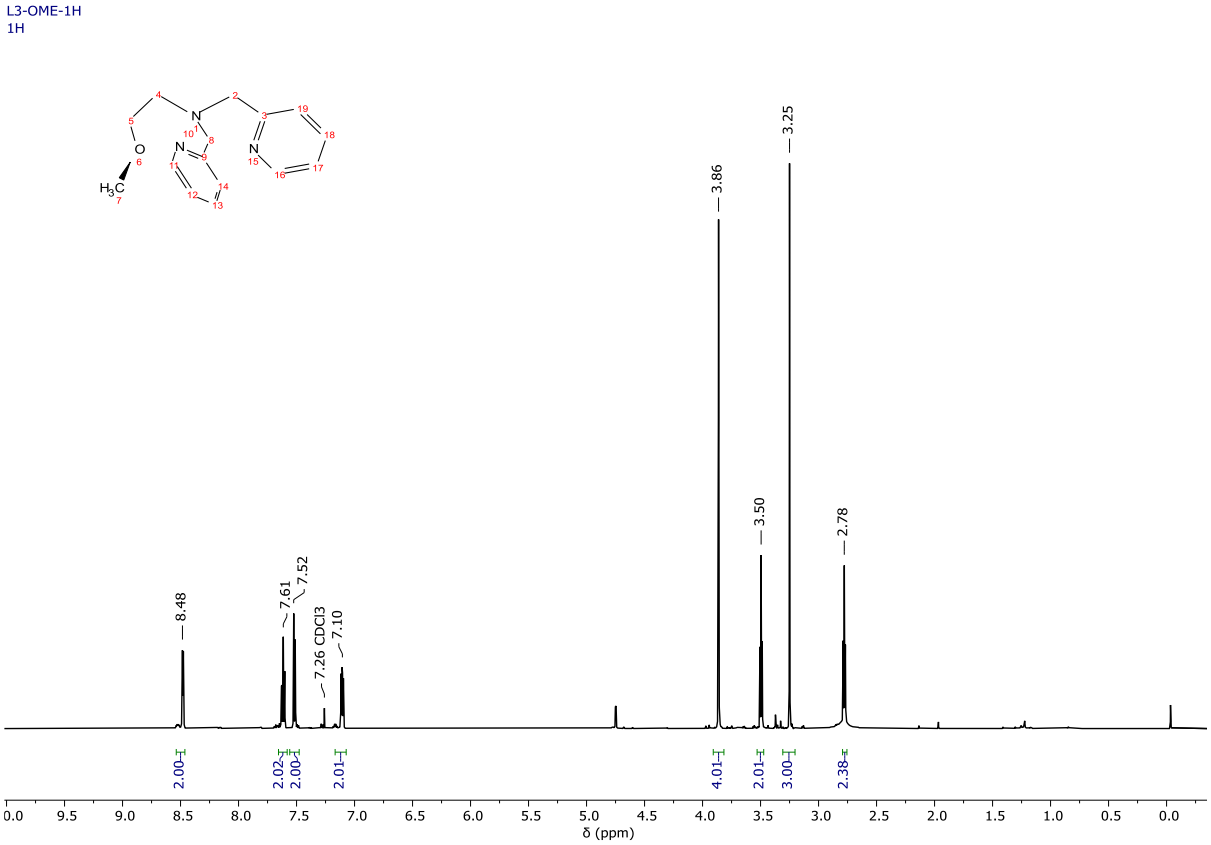

Fig. S3. ^{1}H-NMR (600MHz, $CDCl_3$) spectrum of the ligand N3O.

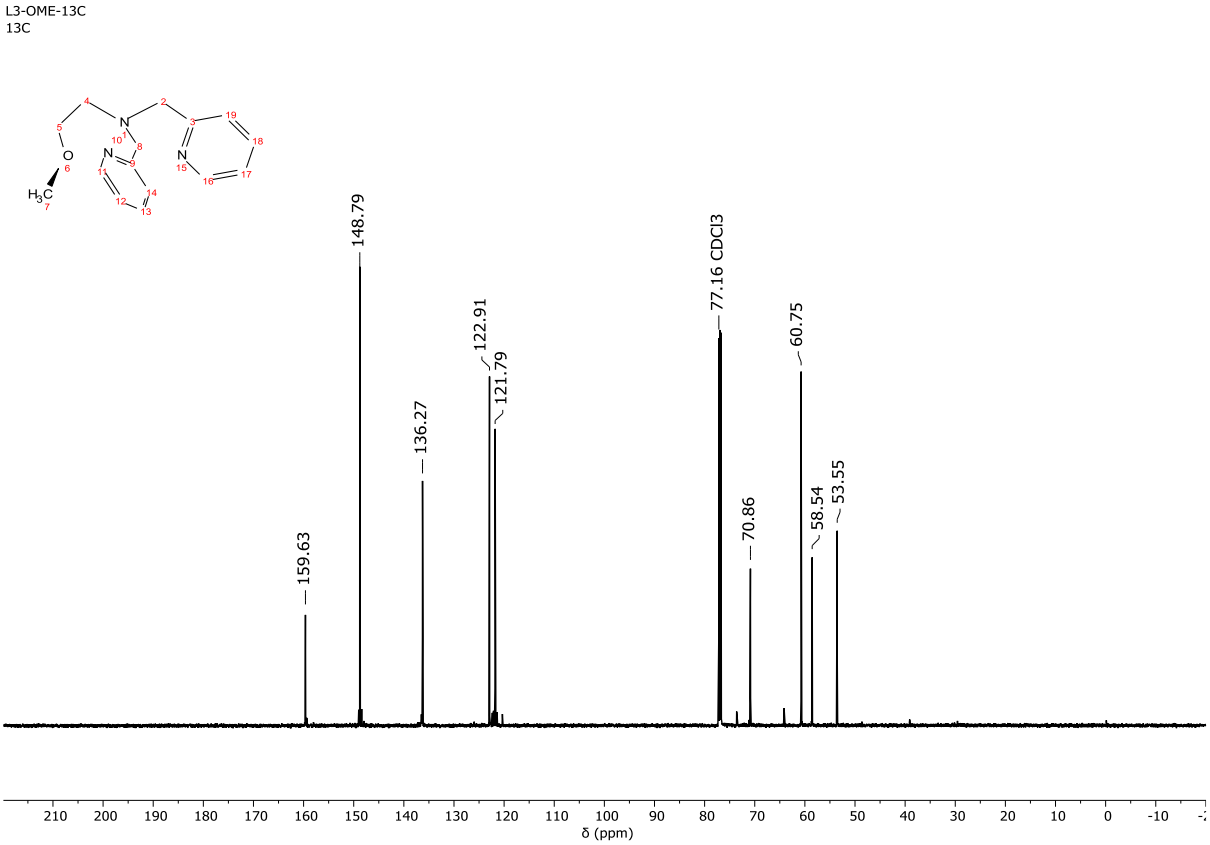

Fig. S4. $^{13}C\{^{1}H\}$ NMR (125MHz, $CDCl_3$) spectrum of the ligand N3O.

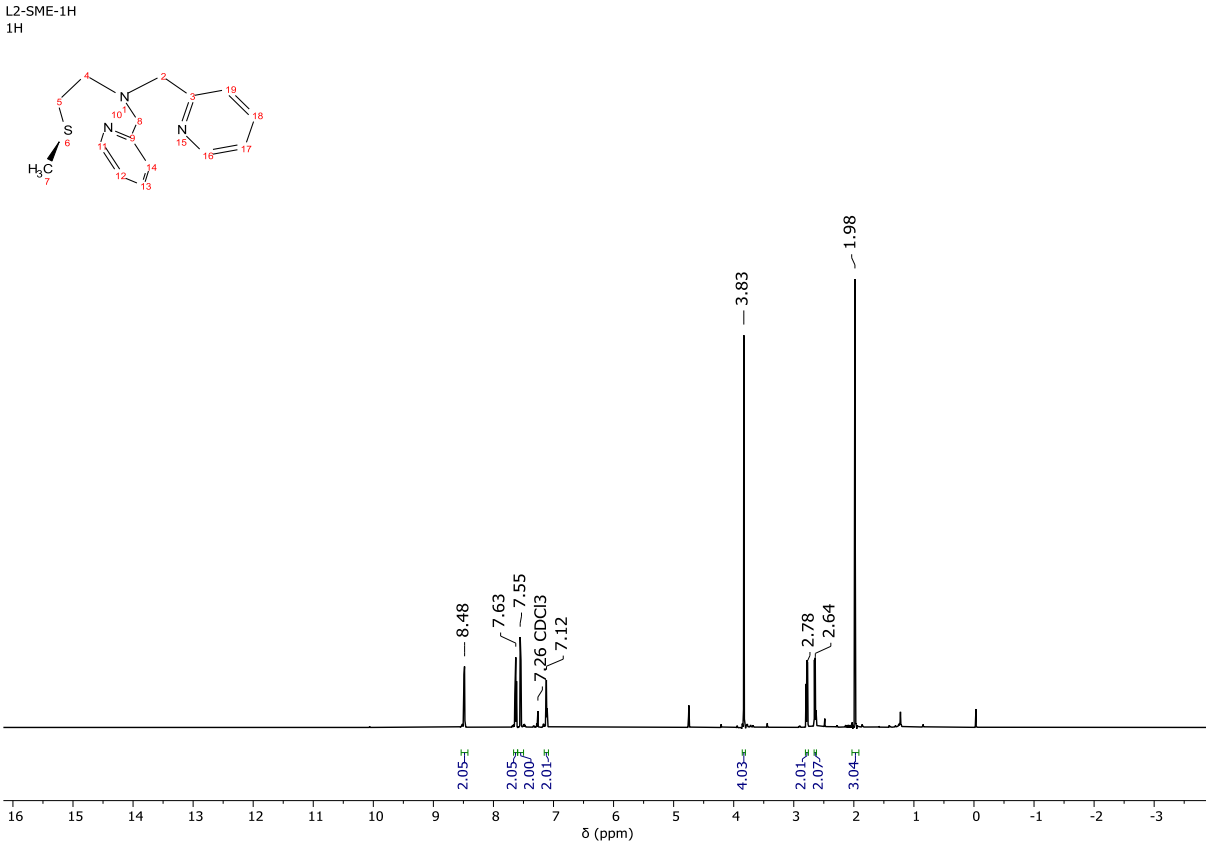

Fig. S5. ^{1}H-NMR (600MHz, $CDCl_3$) spectrum of the ligand N3S .

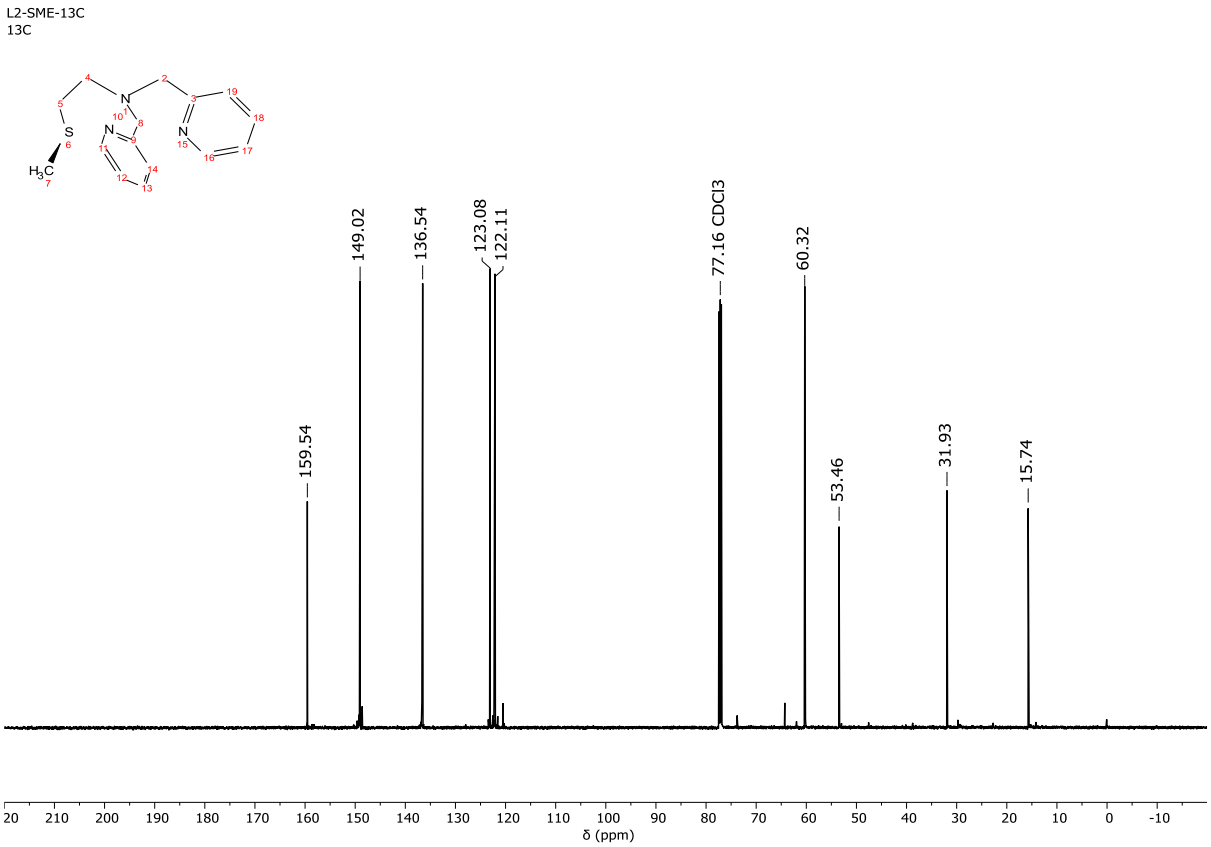

Fig. S6. $^{13}C\{^{1}H\}$ NMR (125MHz, $CDCl_3$) spectrum of the ligand N3S.

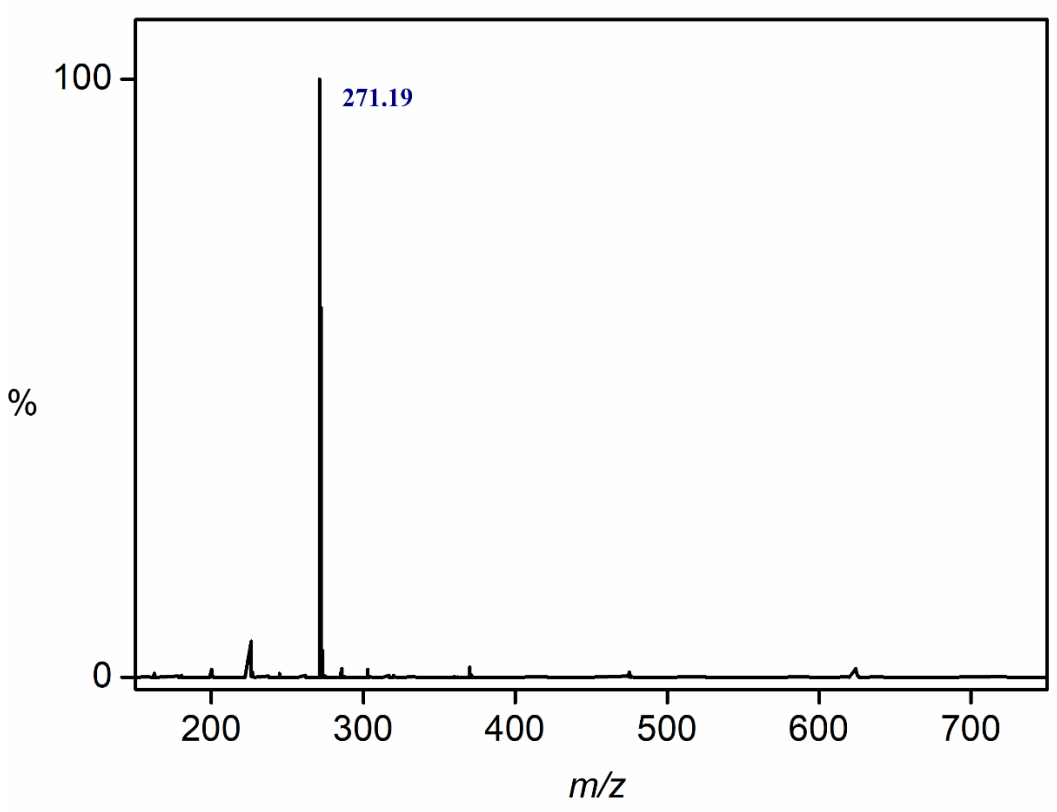

Fig. S7. Positive ESI-MS of the ligand N4 (expected mass 271.17).

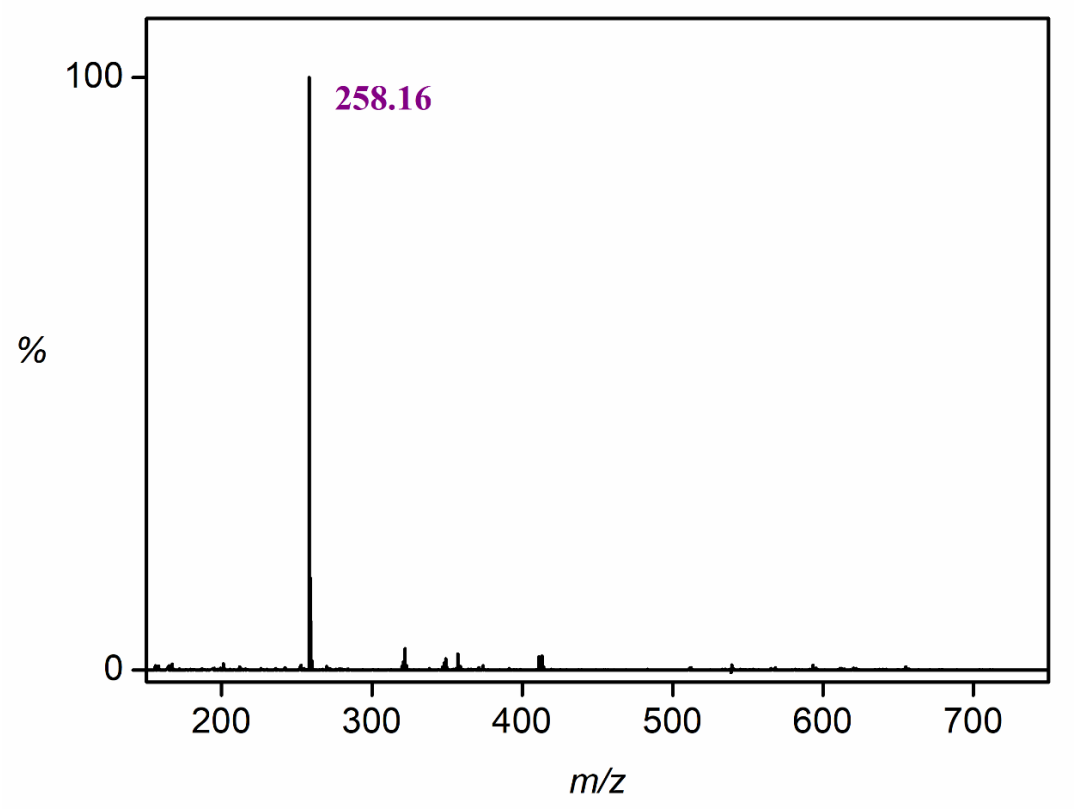

Fig. S8. Positive ESI-MS of the ligand N3O (expected mass 258.15).

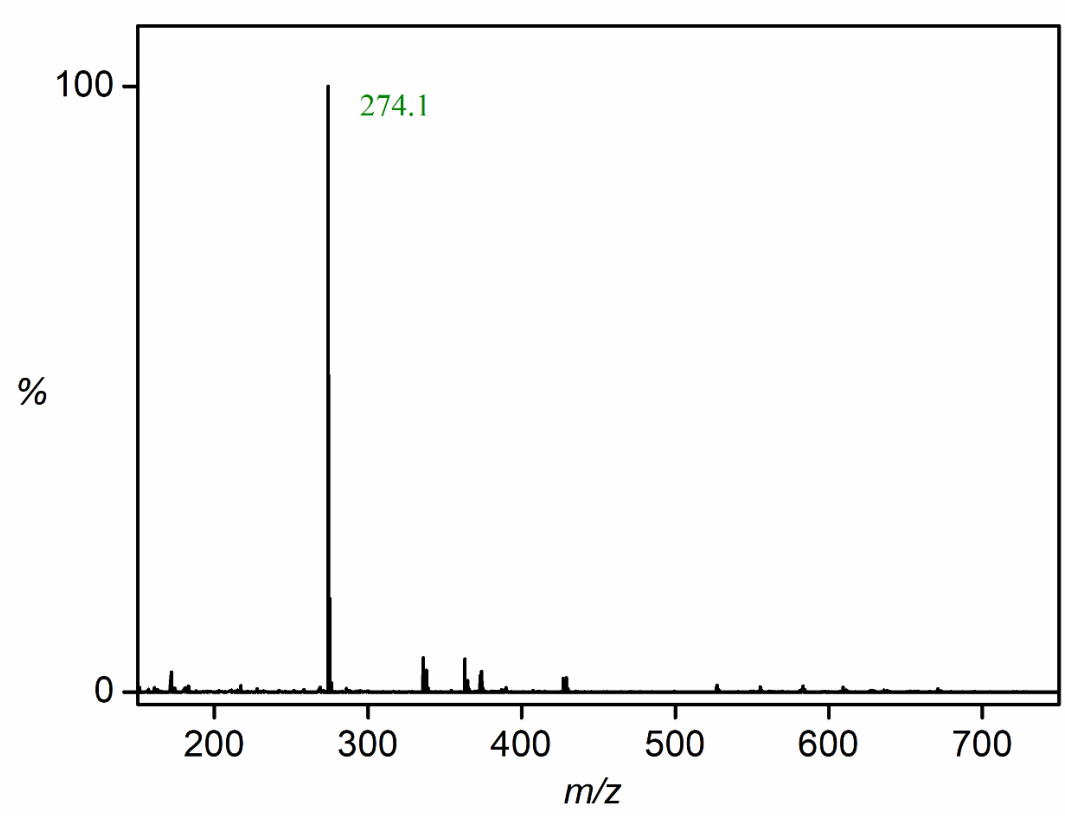

Fig. S9. Positive ESI-MS of the ligand N3S (expected mass 274.13).

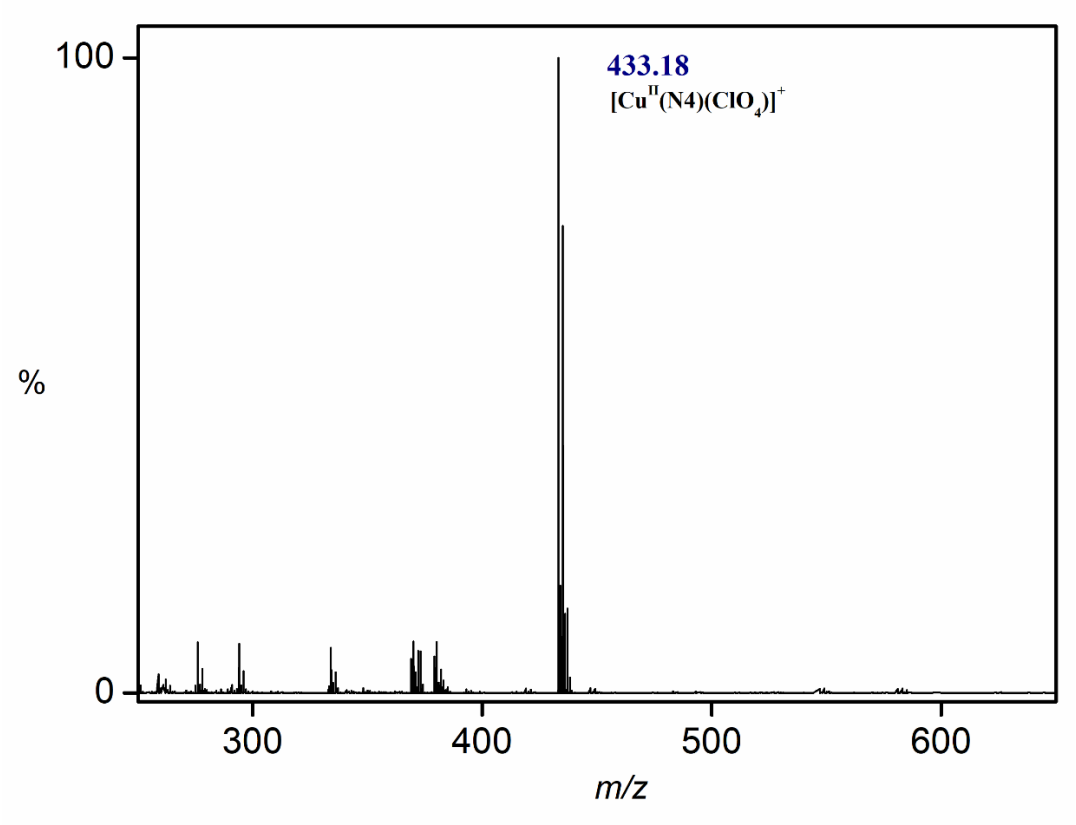

Fig. S10. Positive ESI-MS of complex **1**, *m/z* = 433.58 corresponds to $[Cu^{II}(N4)(ClO_4)]^+$ in CH_3CN at 298 K.

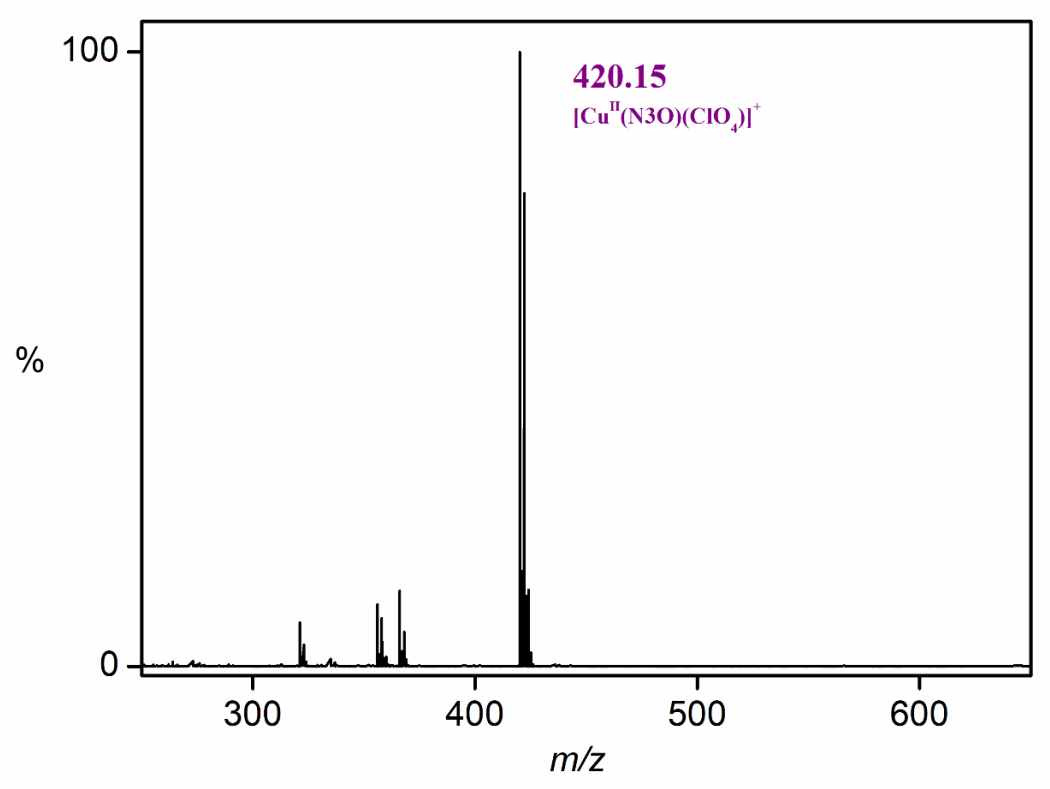

Fig. S11. Positive ESI-MS of complex **2**, *m/z* 420.15 corresponds to $[Cu^{II}(N3O)(ClO_4)]^+$ in CH_3CN at 298 K.

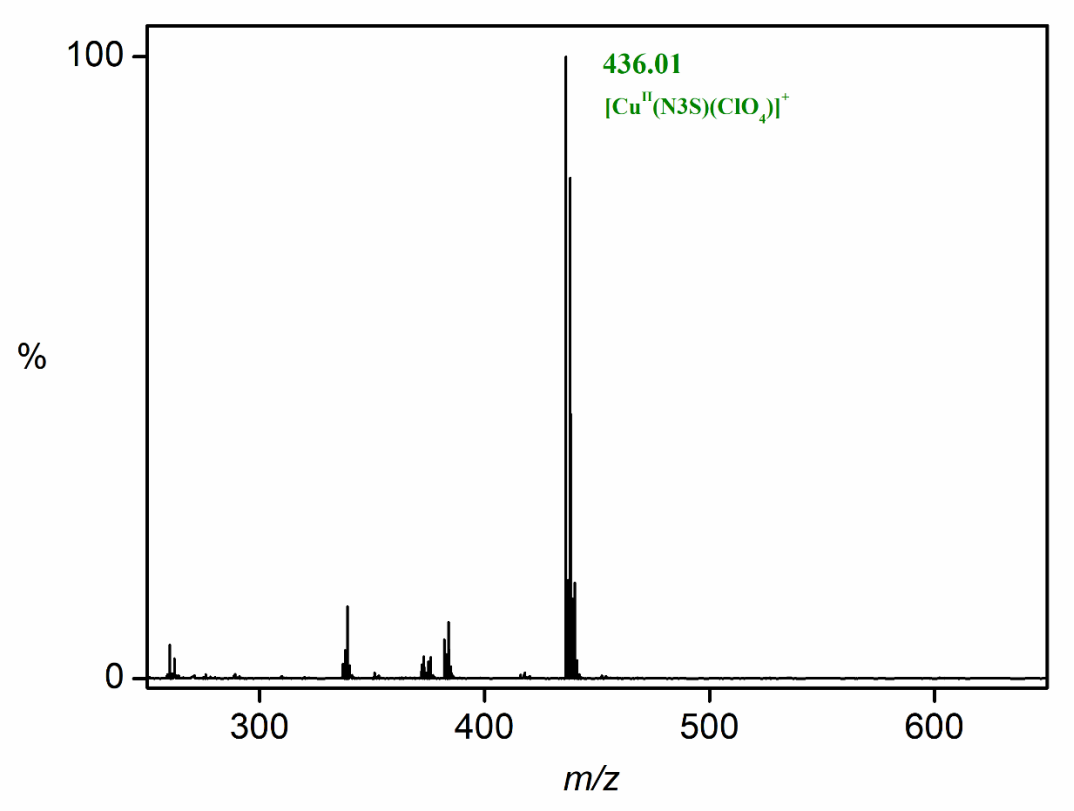

Fig. S12. Positive ESI-MS of complex **3**, *m/z* 436.01 corresponds to $[Cu^{II}(N3S)(ClO_4)]^+$ in CH_3CN at 298 K.

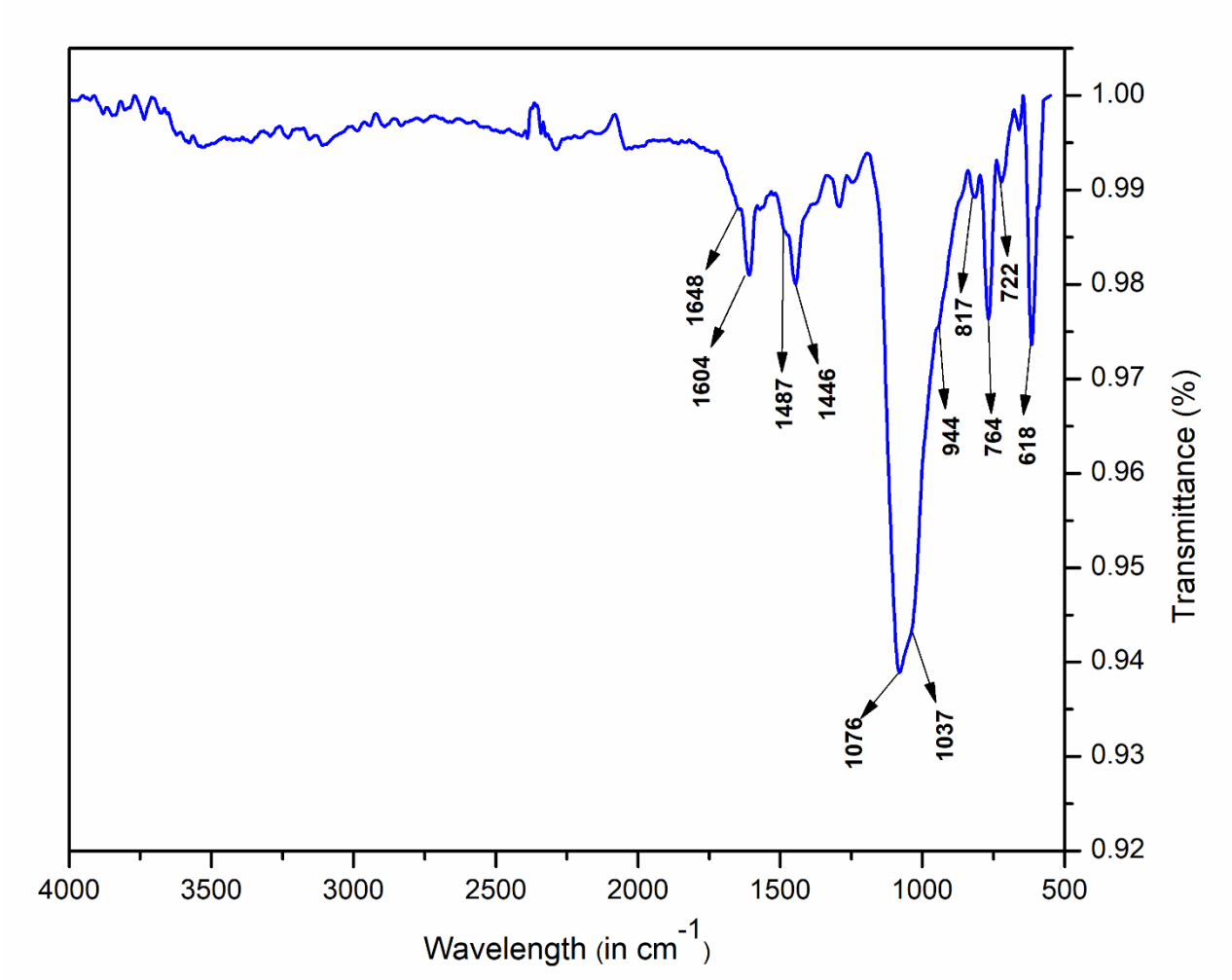

Fig. S13. FT-IR Spectra of Complex **1.**

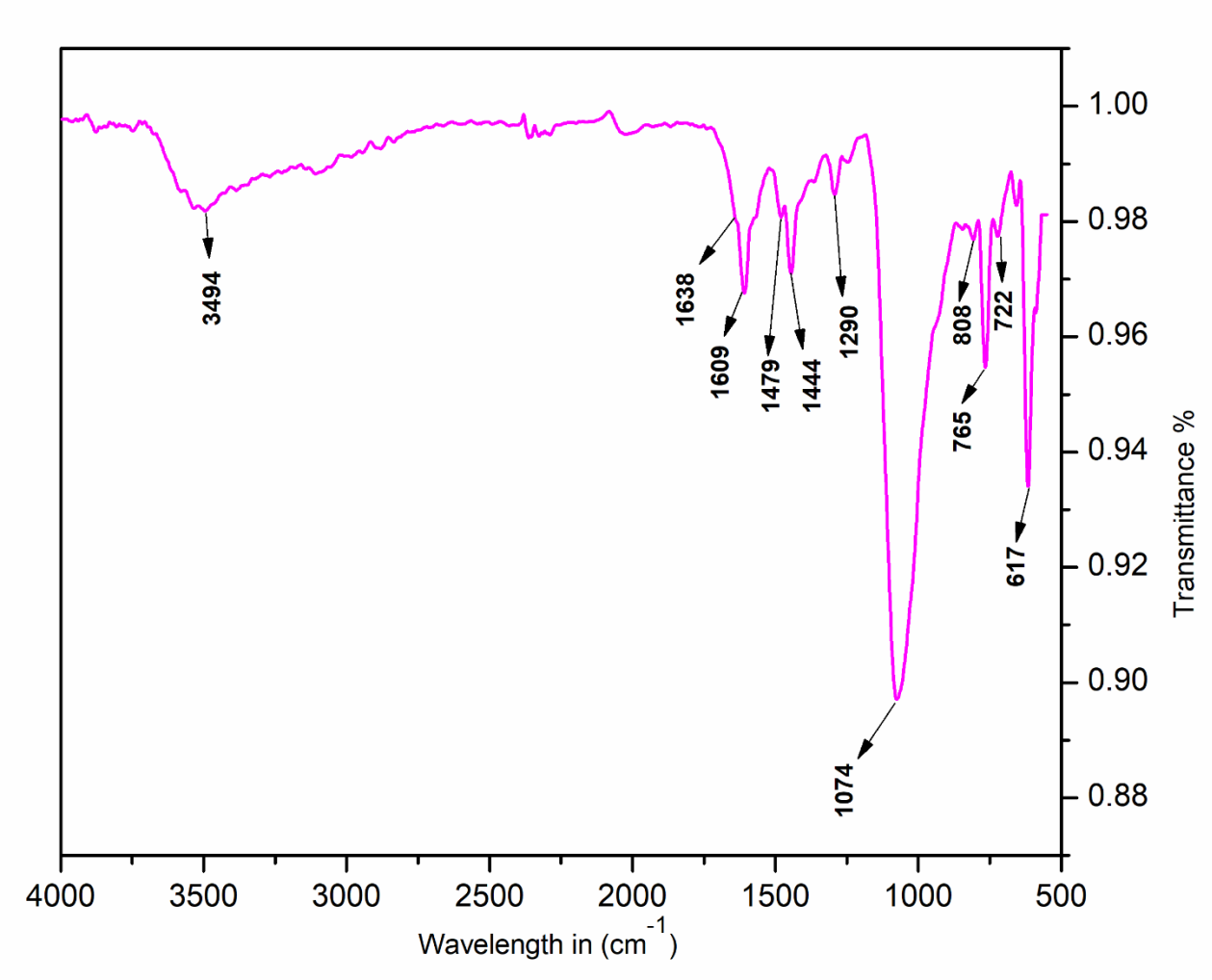

Fig. S14. FT-IR Spectra of Complex **2**.

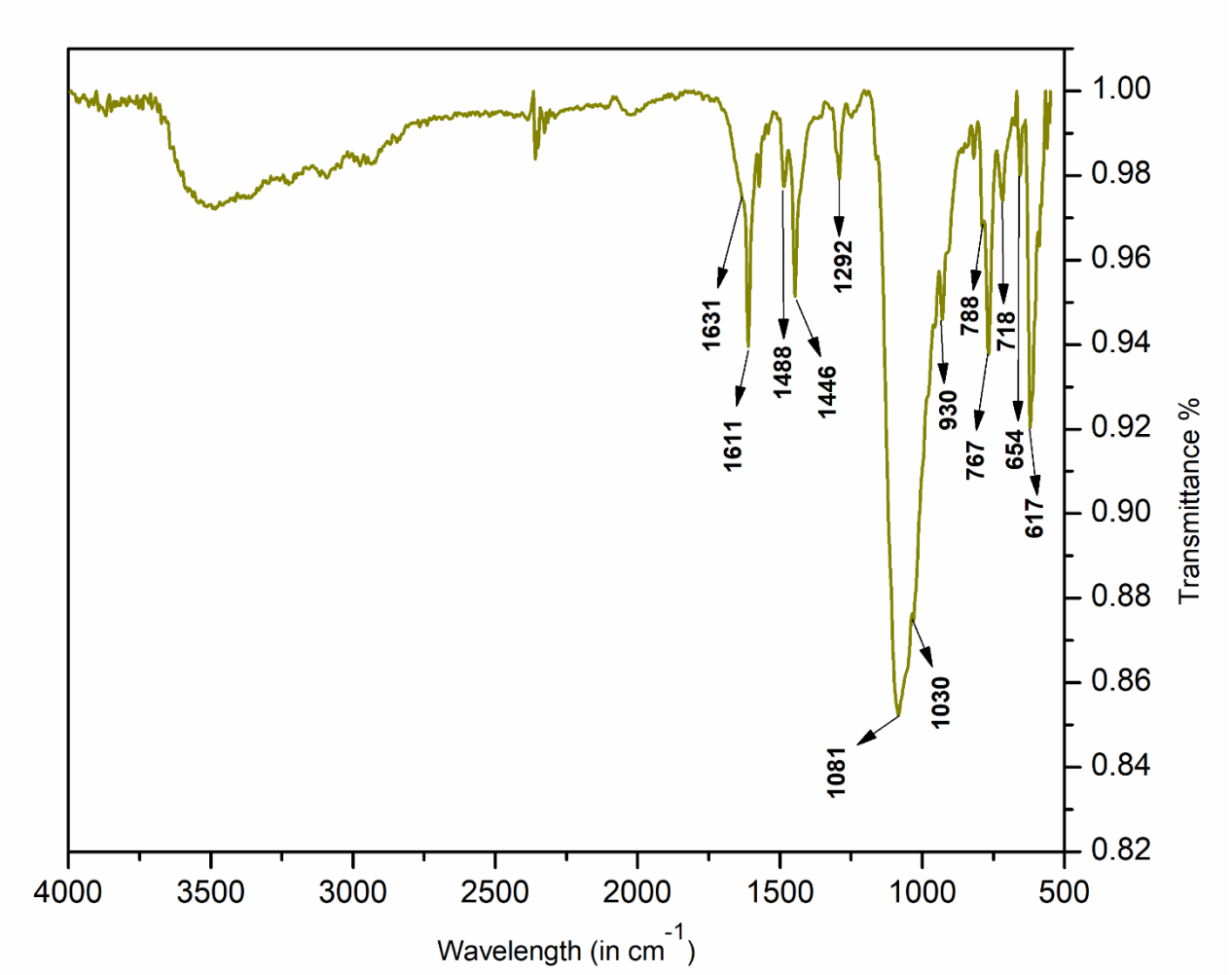

Fig. S15. FT-IR Spectra of Complex **3.**

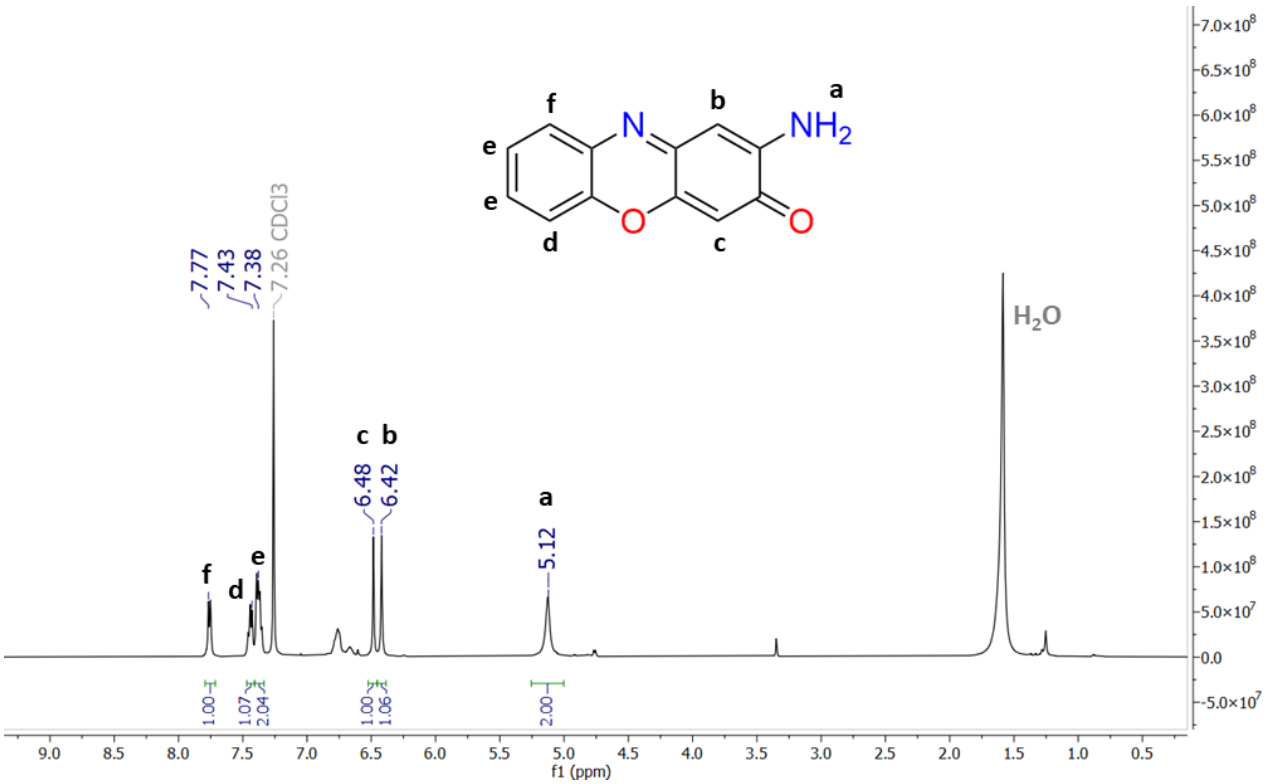

Fig. S16. ^{1}H-NMR (500 MHz, $CDCl_3$) of the product (APX) obtained. Peaks are assigned based on reported data.[52,81]

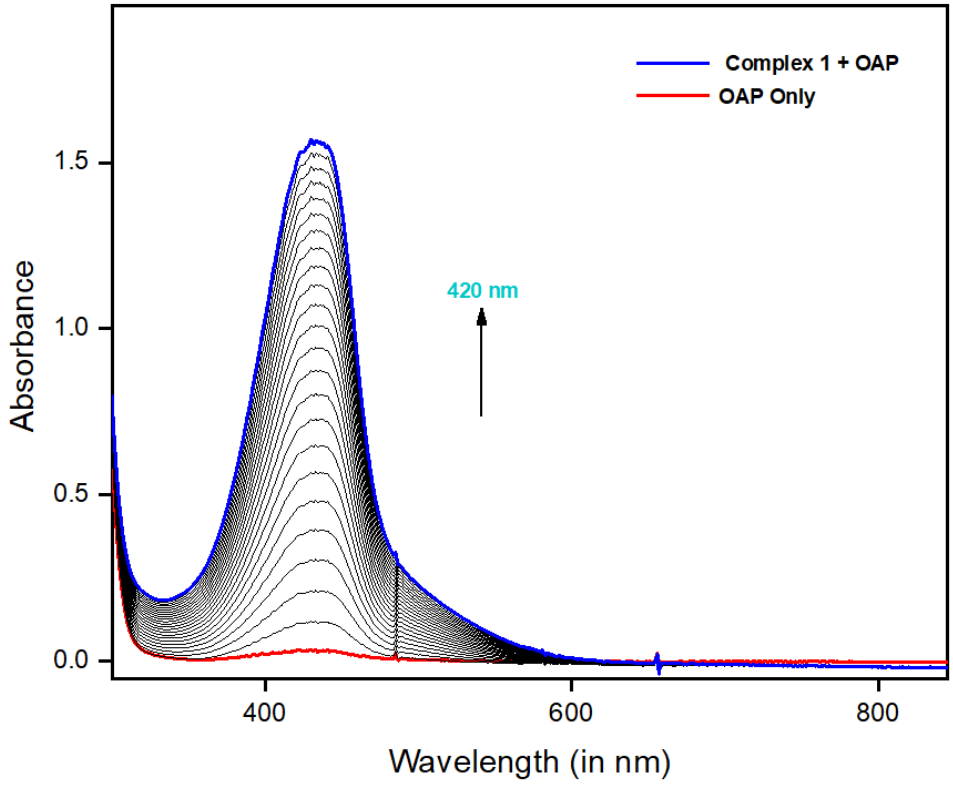

Fig. S17. Phenoxazinone chromophore formation UV band at 440 nm due to aerobic oxidation of OAP in the presence of complex **1** (Conditions: $[Complex]_0 = 2.5 \times 10^{-5}$ M and $[OAP]_0 = 3.75 \times 10^{-3}$ M) in HEPES Buffer (pH 7.4, 25°C).

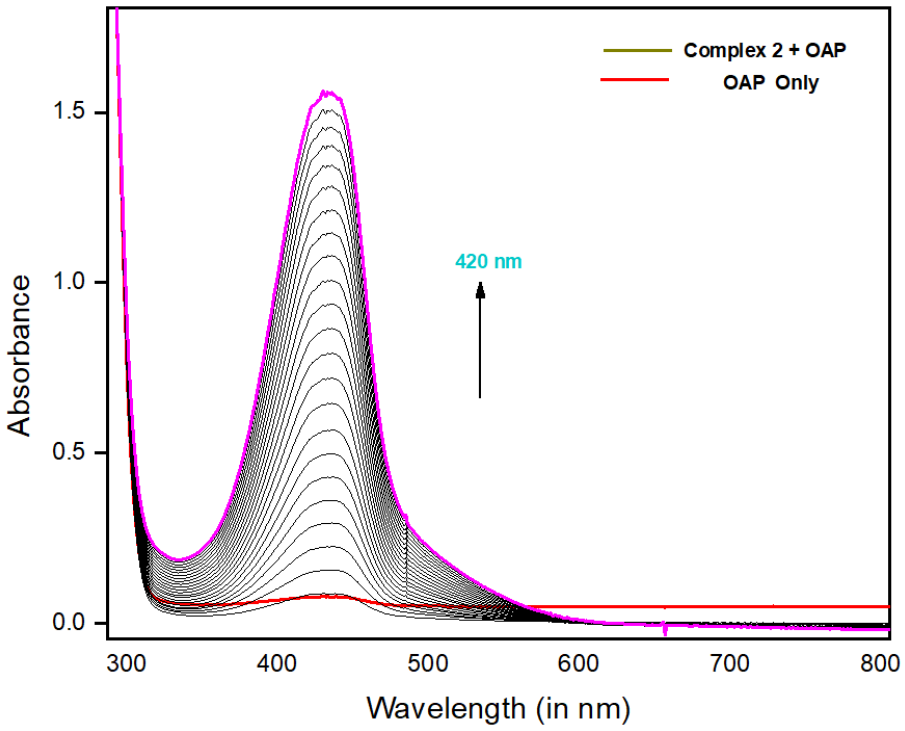

Fig. S18. Phenoxazinone chromophore formation UV band at 440 nm due to aerobic oxidation of OAP in the presence of complex **3** (Conditions: $[Complex]_0 = 2.5 \times 10^{-5}$ M and $[OAP]_0 = 3.75 \times 10^{-3}$ M) in HEPES Buffer (pH 7.4, 25°C).

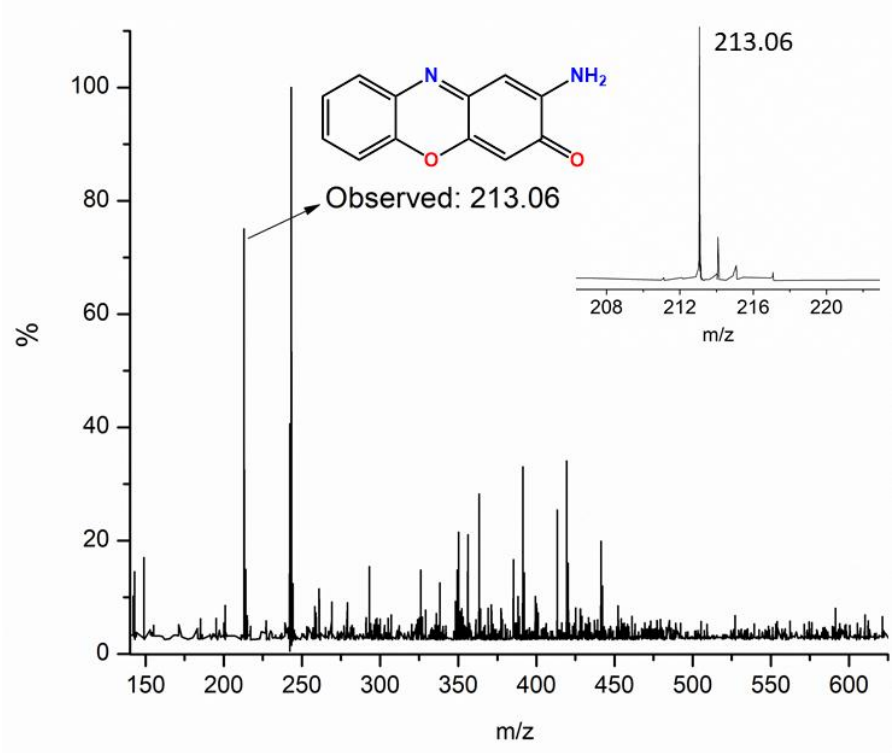

Fig. S19. HRMS of the product (APX) formed. Inset shows the isotopic distribution pattern for the peak at *m/z* 213.06.

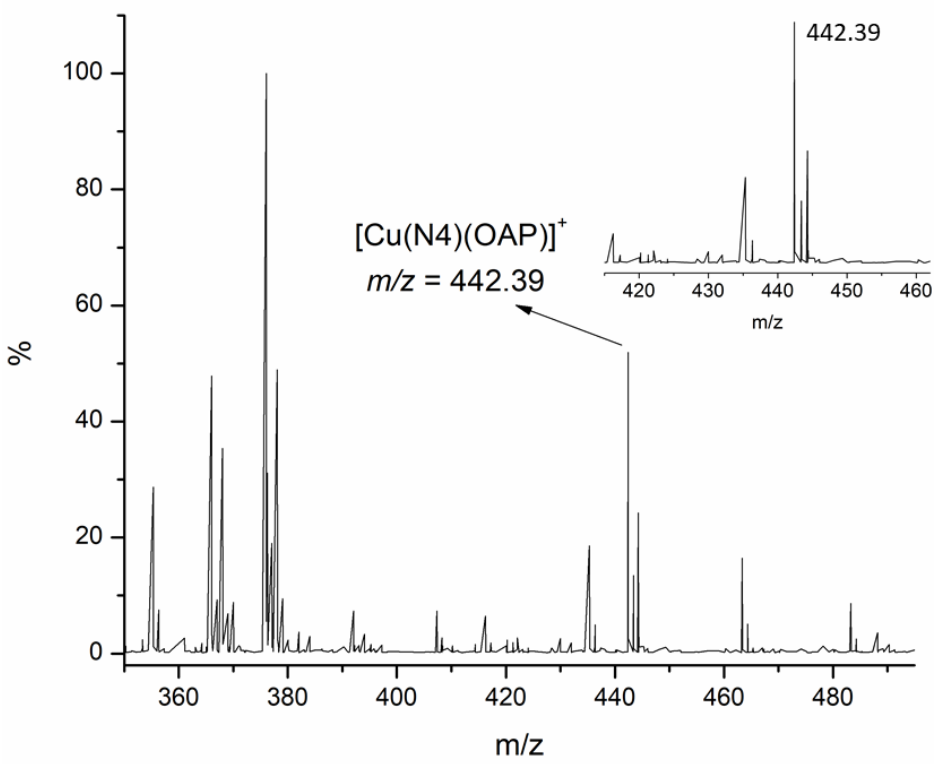

Fig. S20. HRMS of the complex-substrate adduct, peak at *m/z* 442.39 corresponds to the binding of OAP to the Cu centre in **1**. Inset shows the isotopic distribution pattern for the peak at *m/z* 442.39.

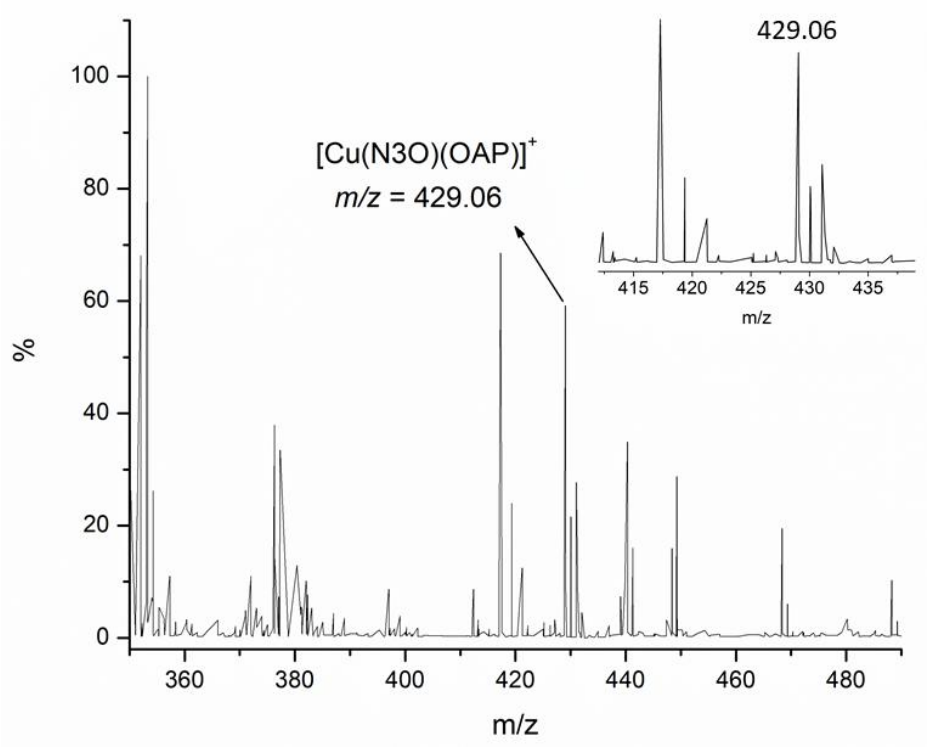

Fig. S21. HRMS of the complex-substrate adduct, peak at *m/z* 429.06 corresponds to the binding of OAP to the Cu centre in **2**. Inset shows the isotopic distribution pattern for the peak at *m/z* 429.06.

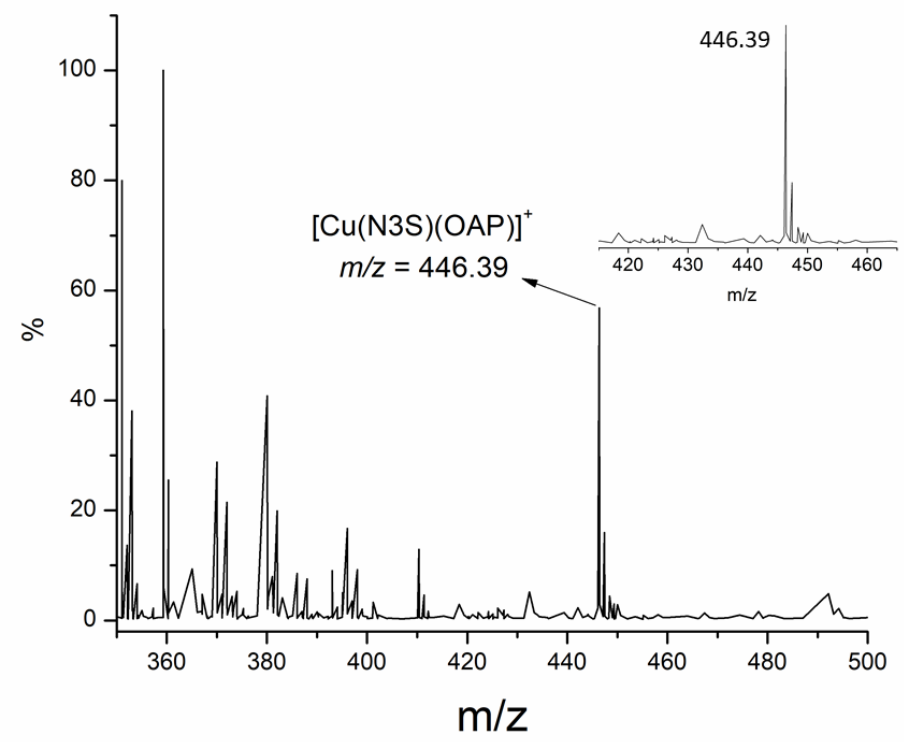

Fig. S22. HRMS of the complex-substrate adduct, peak at *m/z* 446.39 corresponds to the binding of OAP to the Cu centre in **3**. Inset shows the isotopic distribution pattern for the peak at *m/z* 446.39.

Table S1. SHAPE parameter of **1**, **2** and **3**.

Complexes	JTBPY-5 (D_{3h})	SPY-5 (C_{4v})	TBPY-5 (D_{3h})	vOC-5 (C_{4v})	PP-5 (D_{5h})
1	5.842	1.146	3.091	1.713	32.676
3	7.592	1.484	4.126	2.739	31.334
	JPPY-6 (C_{5v})	TPR-6 (D_{3h})	OC-6 (Oh)	PPY-6 (C_{5v})	HP-6 (D_{6h})
2	26.573	13.362	1.528	23.527	31.196

JTBPY-5 = Johnson trigonal bipyramid J12, SPY-5 = Spherical square pyramid, TBPY-5 = Trigonal bipyramid, vOC-5 = Vacant octahedron, PP-5 = Pentagon, vTBPY-4 = Vacant trigonal bipyramid, SS-4 = Seesaw, T-4 = Tetrahedron, SP-4 = Square. JPPY-6 =Johnson pentagonal pyramid J2, TPR-6 = Trigonal prism, OC-6 = Octahedron, PPY-6 = Pentagonal pyramid, HP-6 = Hexagon

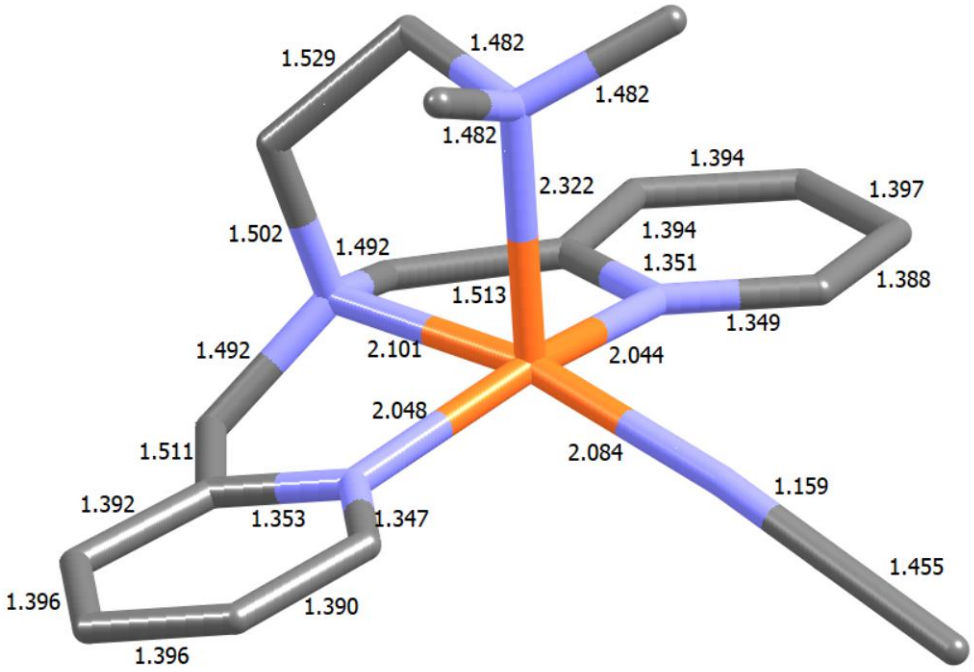

Fig. S23. Optimized geometry of **1** with selected bond length (Å). Hydrogen atoms are omitted for clarity.

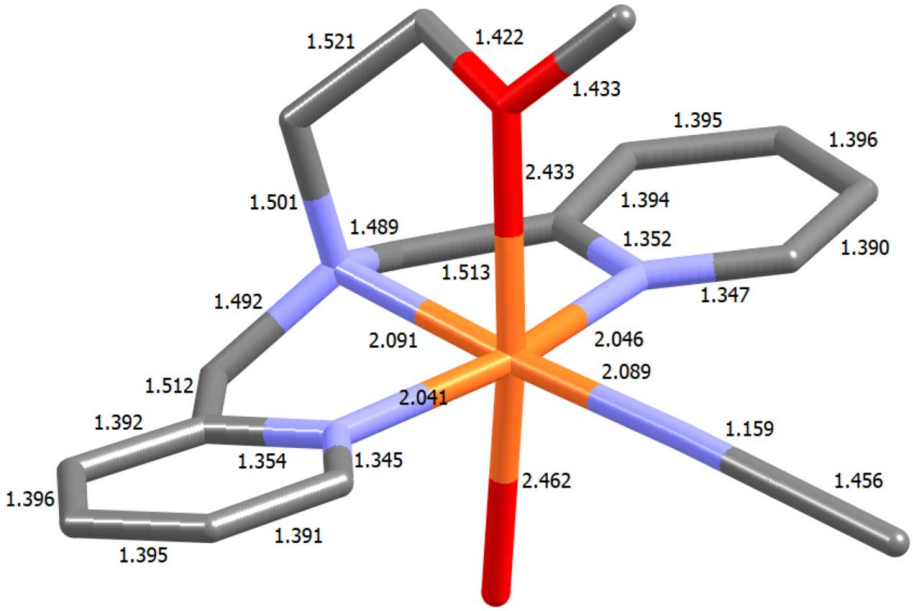

Fig. S24. Optimized geometry of **2** with selected bond length (Å). Hydrogen atoms are omitted for clarity.

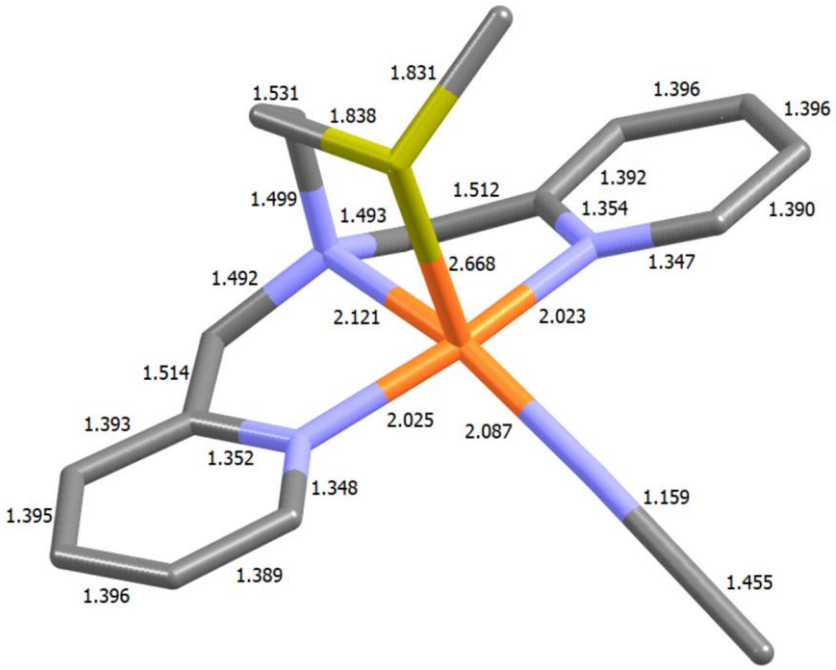

Fig. S25. Optimized geometry of **3** with selected bond length (Å). Hydrogen atoms are omitted for clarity.

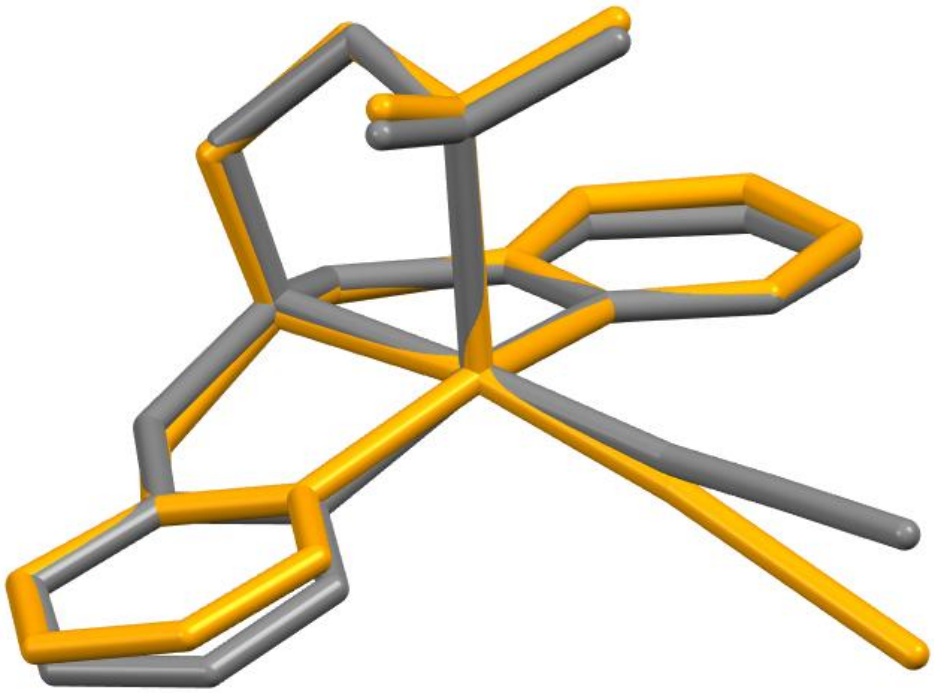

Fig. S26. Overlay plot of complex **1** (Grey, XRD and Orange, DFT). Hydrogen atoms are omitted for clarity.

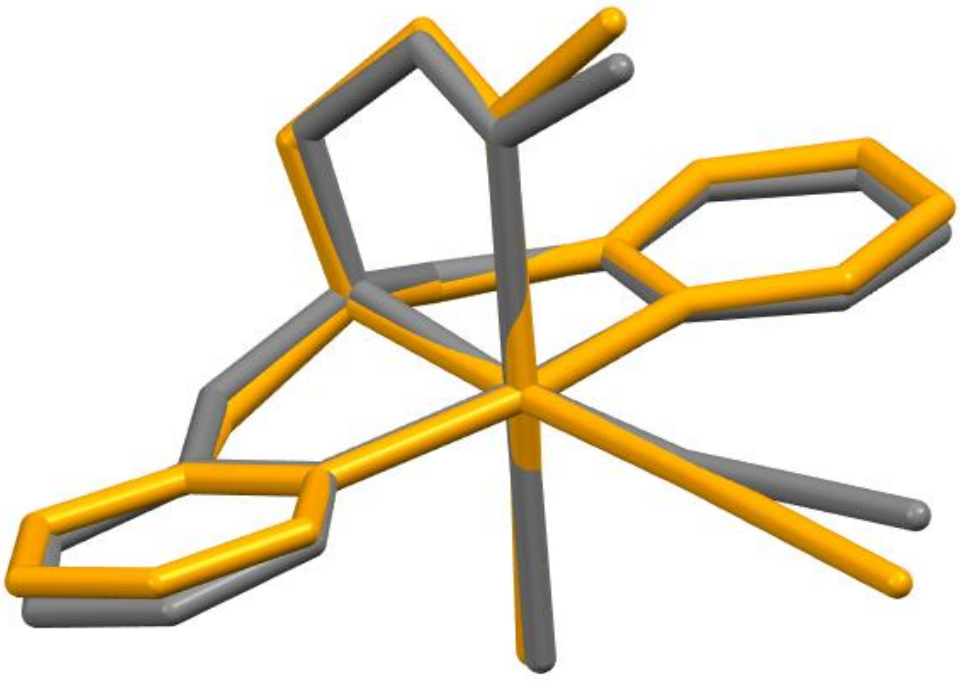

Fig. S27. Overlay plot of complex **2** (Grey, XRD and Orange, DFT). Hydrogen atoms are omitted for clarity.

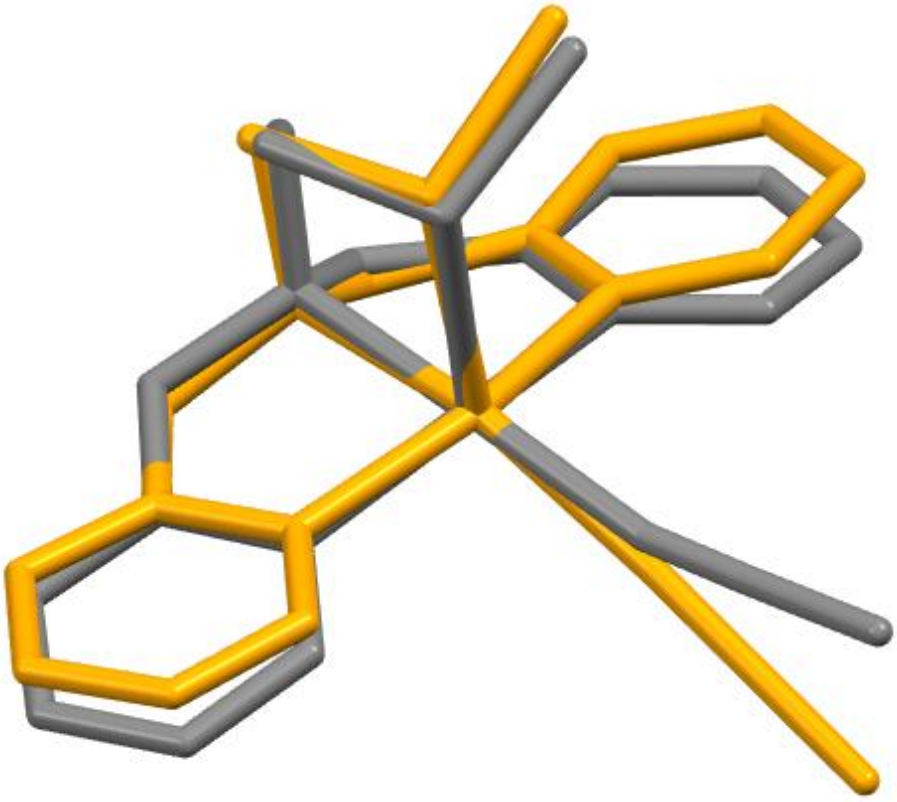

Fig. S28. Overlay plot of complex **3** (Grey, XRD and Orange, DFT). Hydrogen atoms are omitted for clarity.

Table S2. Computed absorption maxima (λ_{max} nm), Electronic excitation energies (E, eV), and Oscillator strength (*f*) of **1, 2** and **3** in solvent phase (acetonitrile).

Complexes	Cal. λ_{max} (nm)	Exp. λ_{max} (nm)	Oscillator Strength f	E (eV)	Main Contributing Configurations
1	784.3	778	0.1151	1.58	HOMO-8 →LUMO(β) (48%) HOMO-16 →LUMO(β) (35%),
	943.9	937	0.0045	1.31	HOMO-15 →LUMO(β) (19%), HOMO-17 →LUMO(β) (15%), HOMO-5 →LUMO(β) (10%), HOMO-3 →LUMO(β) (14%)
2	610.0	623	0.1514	2.03	HOMO-6 →LUMO(B) (59%)
3	626.6	635	0.1492	1.98	HOMO-7 →LUMO(β) (73%)
	770.9	790	0.0064	1.61	HOMO-15 →LUMO(β) (29%), HOMO-14 →LUMO(β) (22%), HOMO-4 →LUMO(β) (18%)

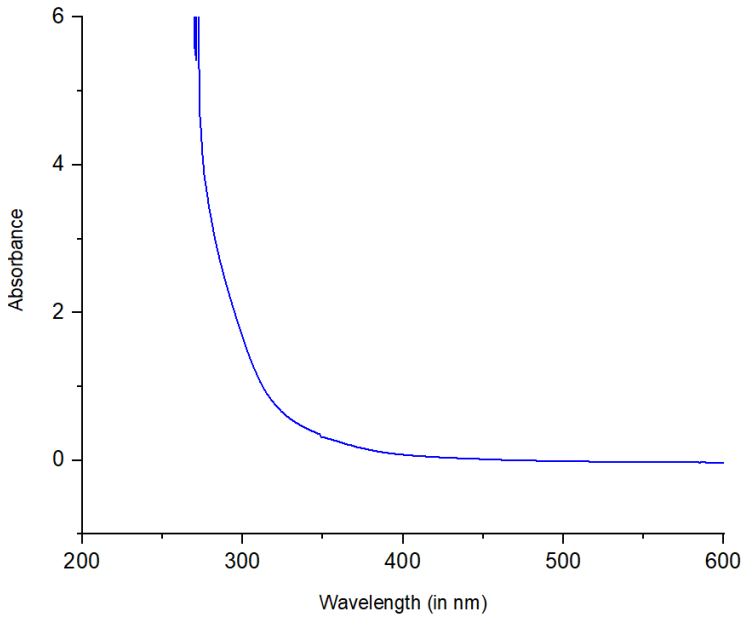

Fig. S29. UV-Vis spectrum obtained after addition of OAP to Cu(II)perchlorate salt; conditions: [Cu-perchlorate]$_0$ = 2.5 × 10^{-5} M and [OAP]$_0$ = 3.75 × 10^{-3} M) in HEPES Buffer (pH 7.4, 25°C).

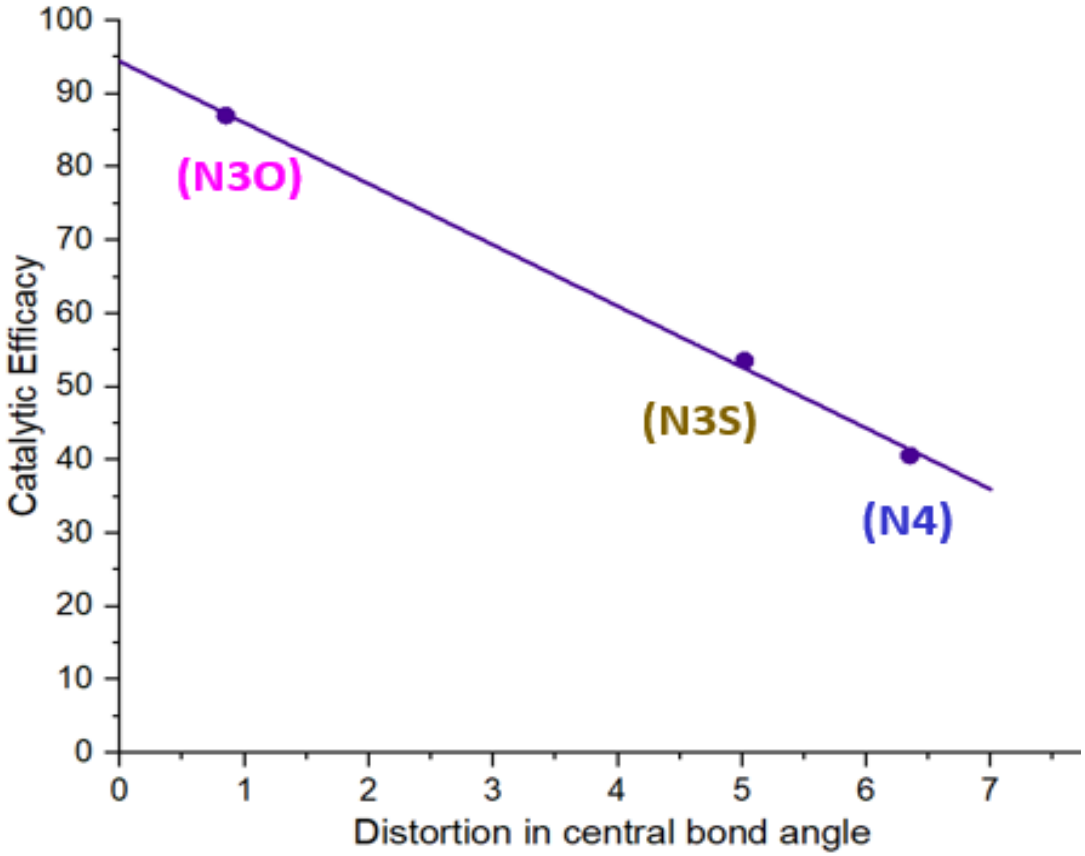

Fig. S30. Plot of correlation between catalytic efficiency with the deviation of the central metal ion from the mean equatorial plane for the complexes **1** (N4), **2** (N3O) and **3** (N3S) for OAP oxidation.

Table S3. Pseudo first-order rate constants determined for the Complexes **1**, **2** and **3** (0.025 mM solution) with OAP at 25 °C in HEPES Buffer.

Substrate Concentration (mM)	Pseudo first-order rate constants (s^{-1})		
	Complex **1**	Complex **2**	Complex **3**
0.25	0.0001864	0.0002180	0.0001899
0.5	0.0002110	0.0002392	0.0003943
0.75	0.0003000	0.0002750	0.0005238
1	0.0003281	0.0002878	0.0005299
1.25	0.0003435	0.0003100	0.0005400

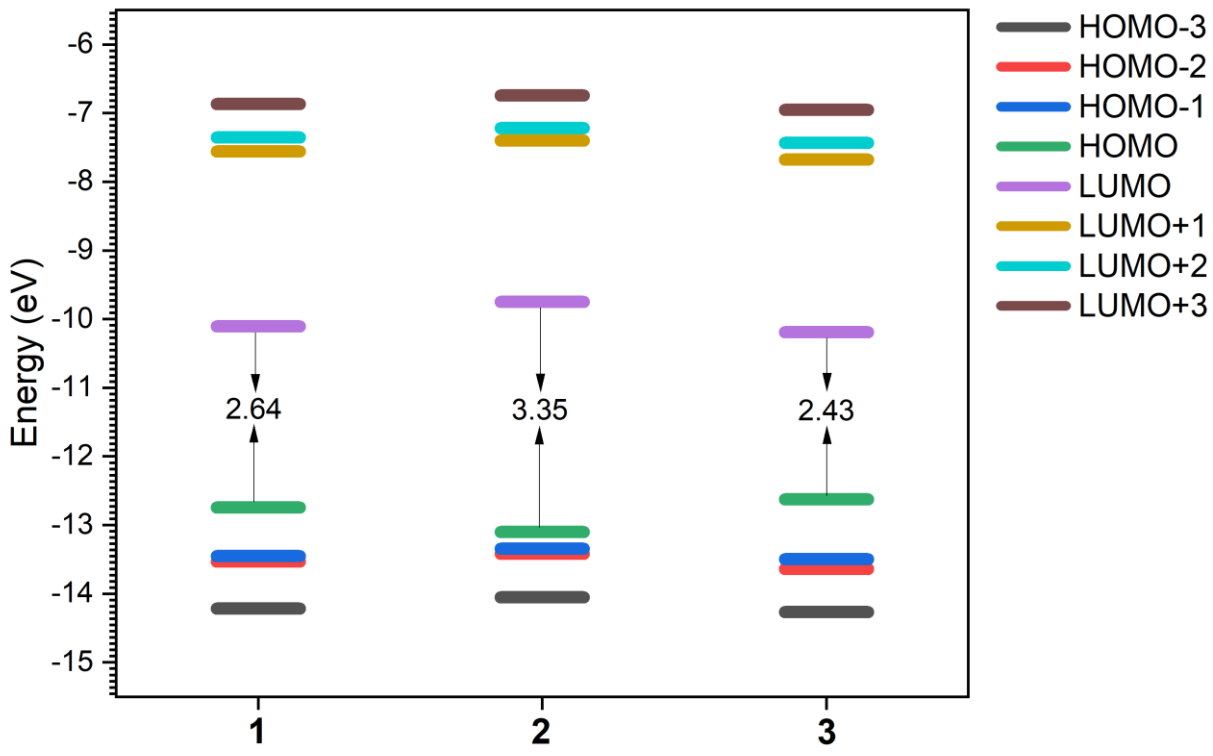

Fig. S31. FMO energy levels of **1**, **2** and **3**.

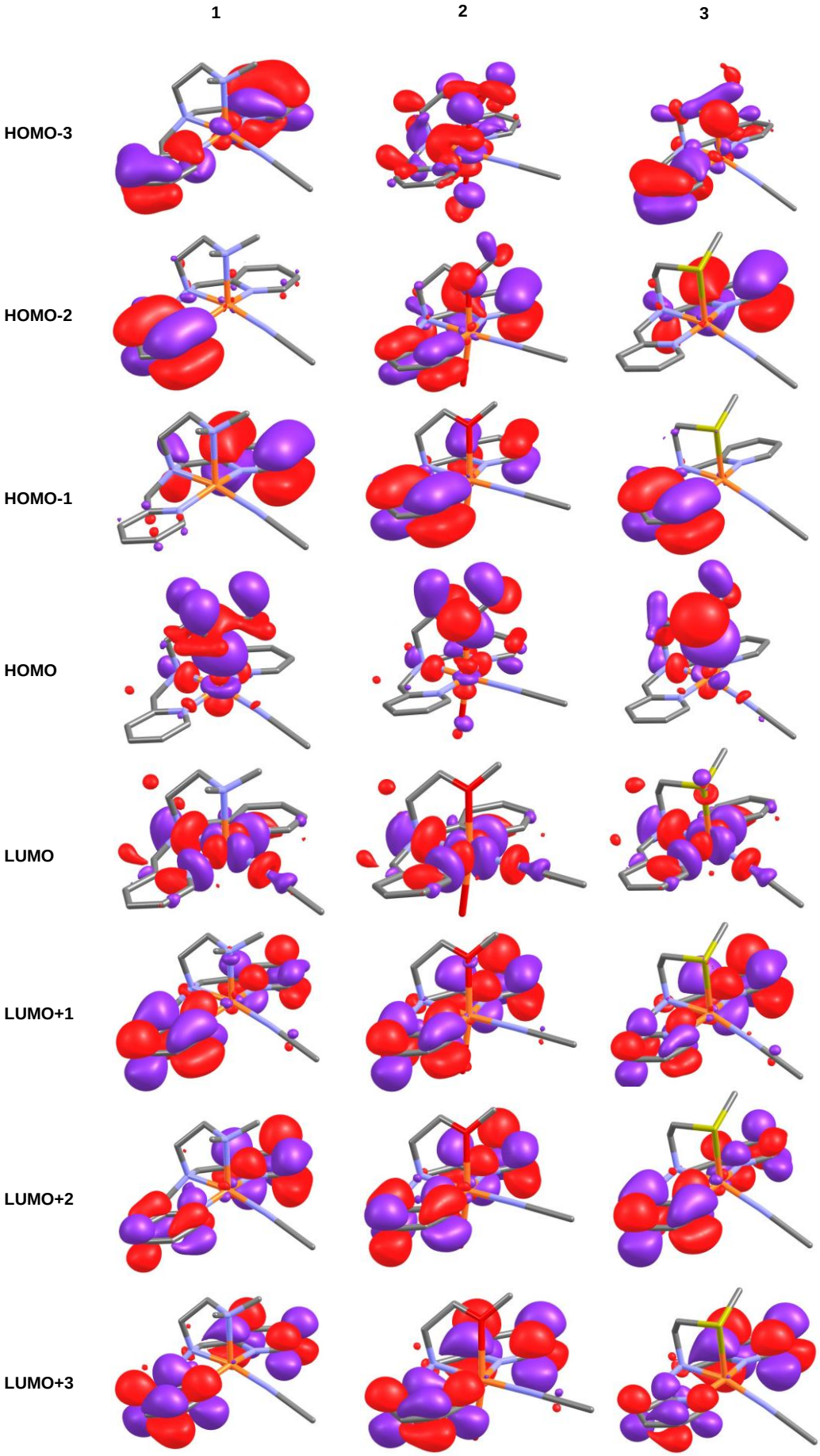

Fig. S32. Highest occupied molecular orbital and lowest unoccupied molecular orbitals of **1**, **2** and **3**.

Table S4. Frontier Molecular Orbital compositions (%) in the ground state for **1**.

	Energy (eV)	Cu1	L	MeCN
HOMO-3	-14.219	10.24	77.15	0.11
HOMO-2	-13.533	0.71	98.68	0.23
HOMO-1	-13.451	0.18	99.73	0.04
HOMO	-12.746	16.04	82.35	0.81
LUMO	-10.108	55.86	31.77	4.67
LUMO+1	-7.561	4.90	76.20	1.33
LUMO+2	-7.357	1.11	91.43	0.12
LUMO+3	-6.867	1.96	95.14	2.54

Table S5. Frontier Molecular Orbital compositions (%) in the ground state for **2**.

	Energy (eV)	Cu1	L	MeCN	H_2O
HOMO-3	-14.055	33.3	57.4	0.29	9.02
HOMO-2	-13.416	0.96	98.88	0.07	0.08
HOMO-1	-13.343	0.33	99.51	0.03	0.13
HOMO	-13.103	7.56	90.96	0.29	1.20
LUMO	-9.75	56.75	38.72	4.37	0.16
LUMO+1	-7.40	2.74	94.67	0.78	1.80
LUMO+2	-7.221	0.83	99.09	0.04	0.05
LUMO+3	-6.744	3.02	95.86	1.00	0.11

Table S6. Frontier Molecular Orbital compositions (%) in the ground state for **3**.

	Energy (eV)	Cu1	L	MeCN
HOMO-3	-14.267	6.94	92.97	0.09
HOMO-2	-13.639	0.77	98.93	0.3
HOMO-1	-13.499	0.39	99.48	0.13
HOMO	-12.627	10.5	88.43	1.07
LUMO	-10.193	54.16	41.33	4.51
LUMO+1	-7.678	5.39	93.23	1.37
LUMO+2	-7.436	1.24	98.54	0.22
LUMO+3	-6.954	2.05	94.80	3.15

Table S7. Topological parameters at the bond critical points of the Cu–X (N, O and S) and Cu-N bonds of complexes **1**, **2** and **3**.

Complexes	Bond	ρ(r)	$\nabla^2\rho(r)$	G(r)	H(r)	ε	V(r)	|V(r)|/G(r)
1	Cu1-N1	0.0425	0.0517	0.0477	0.0039	0.0034	0.0438	0.9182
	Cu1-N2	0.0690	0.0873	0.0870	0.0003	0.0035	0.0867	0.9966
	Cu1-N3	0.0739	0.1062	0.1067	-0.0006	0.0581	0.1073	1.0056
	Cu1-N4	0.0732	0.1048	0.1051	-0.0003	0.0626	0.1054	1.0029
	Cu1-N5	0.0403	0.0979	0.0915	0.0064	0.0403	0.0851	0.9301
2	Cu1-O1	0.0277	0.0287	0.0274	0.0014	0.1105	0.0260	0.9489
	Cu1-N2	0.0704	0.0905	0.0908	-0.0003	0.0138	0.0911	1.0033
	Cu1-N3	0.0735	0.1049	0.1057	-0.0009	0.0418	0.1066	1.0085
	Cu1-N4	0.0744	0.1058	0.1071	-0.0013	0.0482	0.1083	1.0112
	Cu1-N5	0.0574	0.0969	0.0904	0.0065	0.0629	0.0839	0.9281
3	Cu1-S1	0.0332	0.0265	0.0270	-0.0005	0.0257	0.0275	1.0185
	Cu1-N2	0.0660	0.0846	0.0832	0.0014	0.0067	0.0817	0.9820
	Cu1-N3	0.0781	0.1102	0.1131	-0.0029	0.0628	0.1160	1.0256
	Cu1-N4	0.0780	0.1091	0.1121	-0.0029	0.0622	0.1150	1.0259
	Cu1-N5	0.0582	0.0976	0.0910	0.0066	0.0342	0.0844	0.9275

Table S8. Kinetic parameters of Phenoxazinone synthase like activities of different mononuclear copper complexes.

Complex no.	Catalysts	Conditions	V_{max} (Ms^{-1})	K_M (M)	k_{cat} (s^{-1})	Reference
1	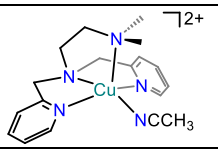	HEPES buffer, pH 7.4, 25°C	4.70×10^{-4}	0.463	18.80	This work
2	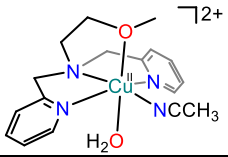	HEPES buffer, pH 7.4, 25°C	3.35×10^{-4}	0.154	13.40	This work
3	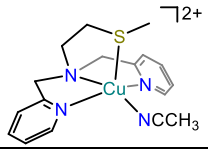	HEPES buffer, pH 7.4, 25°C	8.83×10^{-4}	0.660	35.30	This work
4	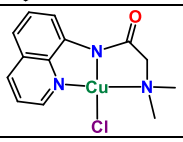	Oxygen saturated MeOH, 60°C	7.47×10^{-7}	0.23	26.94	59
5	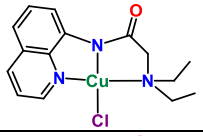	Oxygen saturated MeOH, 60°C	6.8×10^{-7}	0.34	24.72	59
6	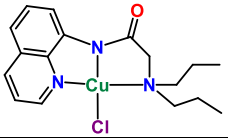	Oxygen saturated MeOH, 60°C	5.86×10^{-7}	0.24	21.11	59
7	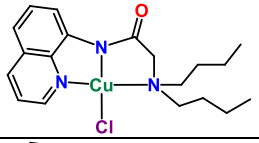	Oxygen saturated MeOH, 60°C	5.38×10^{-7}	0.16	19.16	59
8	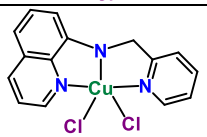	H_2O : MeOH (2:1, v/v), RT	4.35×10^{-8}	14.60×10^{-5}	174×10^{-5}	52
9	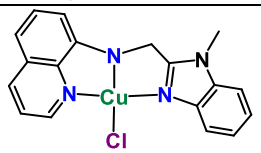	H_2O : MeOH (2:1, v/v), RT	5.33×10^{-8}	13.21×10^{-5}	213×10^{-5}	52
10	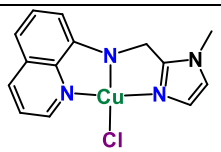	H_2O: MeOH (2:1, v/v), RT	5.85×10^{-8}	5.33×10^{-5}	234×10^{-5}	52
11	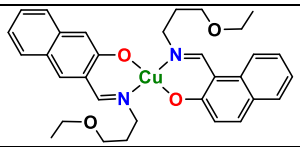	Oxygen saturated MeOH, RT	2.66×10^{-8}	1.19×10^{-3}	2.66×10^{-3}	110
12	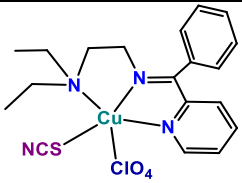	Oxygen saturated MeOH, RT	2.17×10^{-6}	0.02	21.74×10^{-3}	111

13	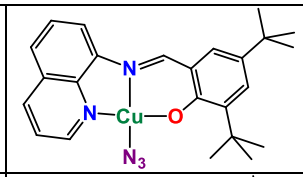	CH_3CN, RT	1.96×10^{-9}	2.97×10^{-3}	3.94×10^{-5}	57
14	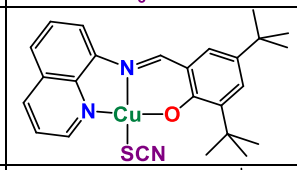	CH_3CN, RT	2.10×10^{-9}	2.96×10^{-3}	4.19×10^{-5}	57
15	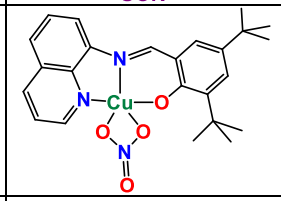	CH_3CN, RT	2.53×10^{-9}	1.95×10^{-3}	5.05×10^{-5}	57
16	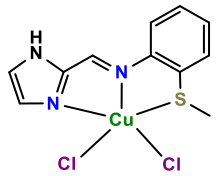	H_2O	5.35×10^{-4}	1.46×10^{-3}	5.33	112
17	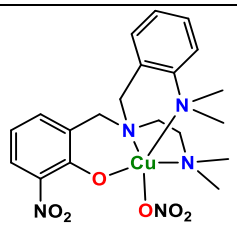	Oxygen saturated water, NEt_3, RT	25.31×10^{-3}	7.5×10^{-3}	253.055	55
18	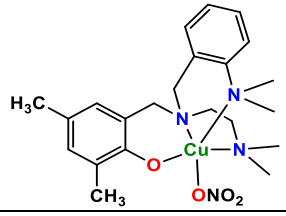	Oxygen saturated water, NEt_3, RT	12.97×10^{-3}	11.67×10^{-3}	129.44	55
19	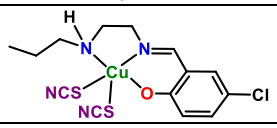	Oxygen saturated DMF, RT	9.38×10^{-7}	8.32×10^{-3}	9.37×10^{-3}	54
20	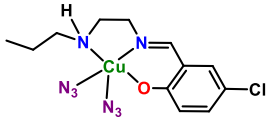	Oxygen saturated DMF, RT	2.68×10^{-8}	2.58×10^{-3}	2.66×10^{-4}	54
21	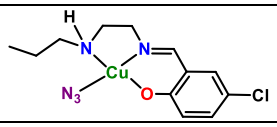	Oxygen saturated DMF, RT	3.73×10^{-6}	4.48×10^{-2}	37.33×10^{-3}	54
22	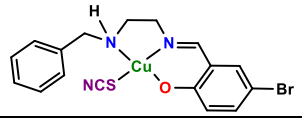	Oxygen saturated MeOH, RT	1.73×10^{-2}	0.45	172.22	56
23	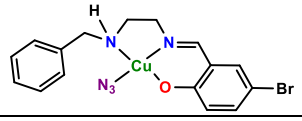	Oxygen saturated MeOH, RT	8.45×10^{-2}	0.73	83.33	56
24	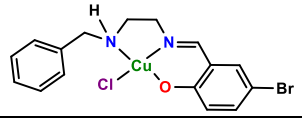	Oxygen saturated MeOH: DMF (19:1), RT	1.05×10^{-2}	1.19	105.55	113

25	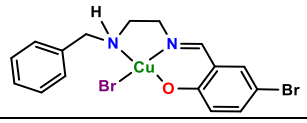	Oxygen saturated MeOH: DMF (19:1), RT	7.2×10^{-3}	0.33	72.22	113
26	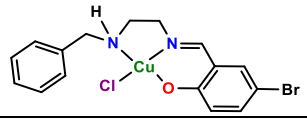	Oxygen saturated MeOH: DMF (19:1), RT	8.9×10^{-2}	1.35	895.00	113
27	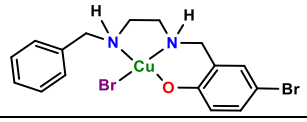	Oxygen saturated MeOH: DMF (19:1), RT	0.05	0.74	500.00	113
28	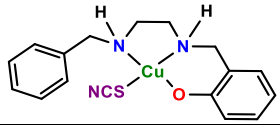	Oxygen saturated MeOH: DMF (19:1), RT	2.3×10^{-3}	0.47	22.77	113
29	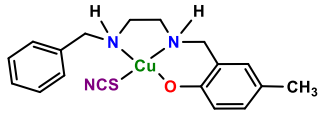	Oxygen saturated MeOH: DMF (19:1), RT	1.8×10^{-3}	0.03	17.50	113
30	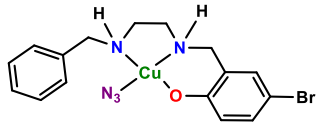	Oxygen saturated MeOH: DMF (19:1), RT	2.6×10^{-3}	0.19	25.83	113
31	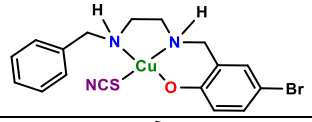	Oxygen saturated MeOH: DMF (19:1), RT	1.1×10^{-2}	0.75	108.33	113
32	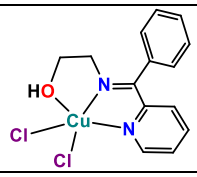	MeOH	2×10^{-5}	-	0.2	62

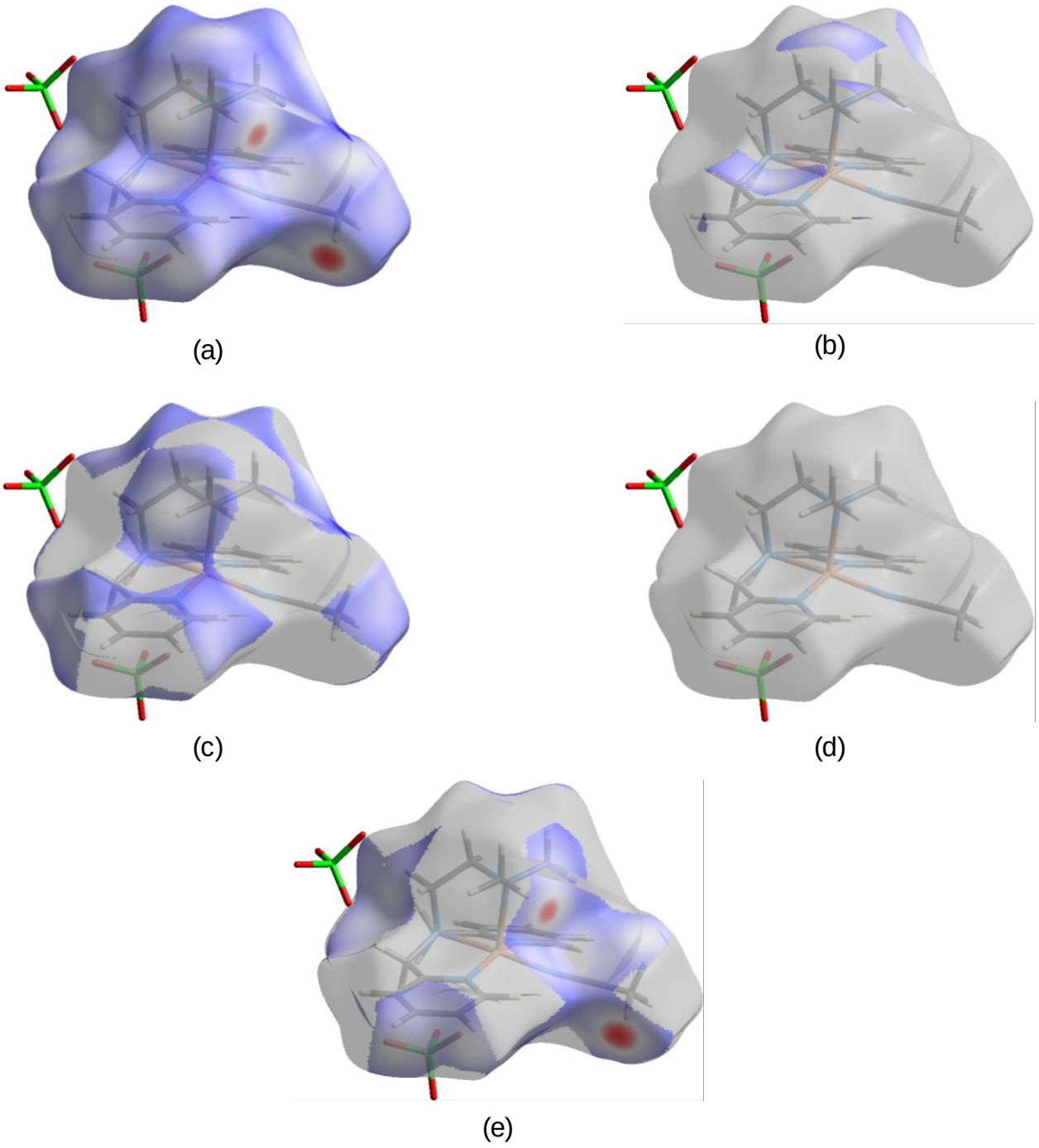

Fig. S33. The Hirshfeld surfaces (**1**) mapped over d_{norm} in the range -0.292 to +0.521 (arbitrary units) for visualizing the weak intermolecular (a) All (b) C···H (c) H···H (d) N···H (d) O···H.

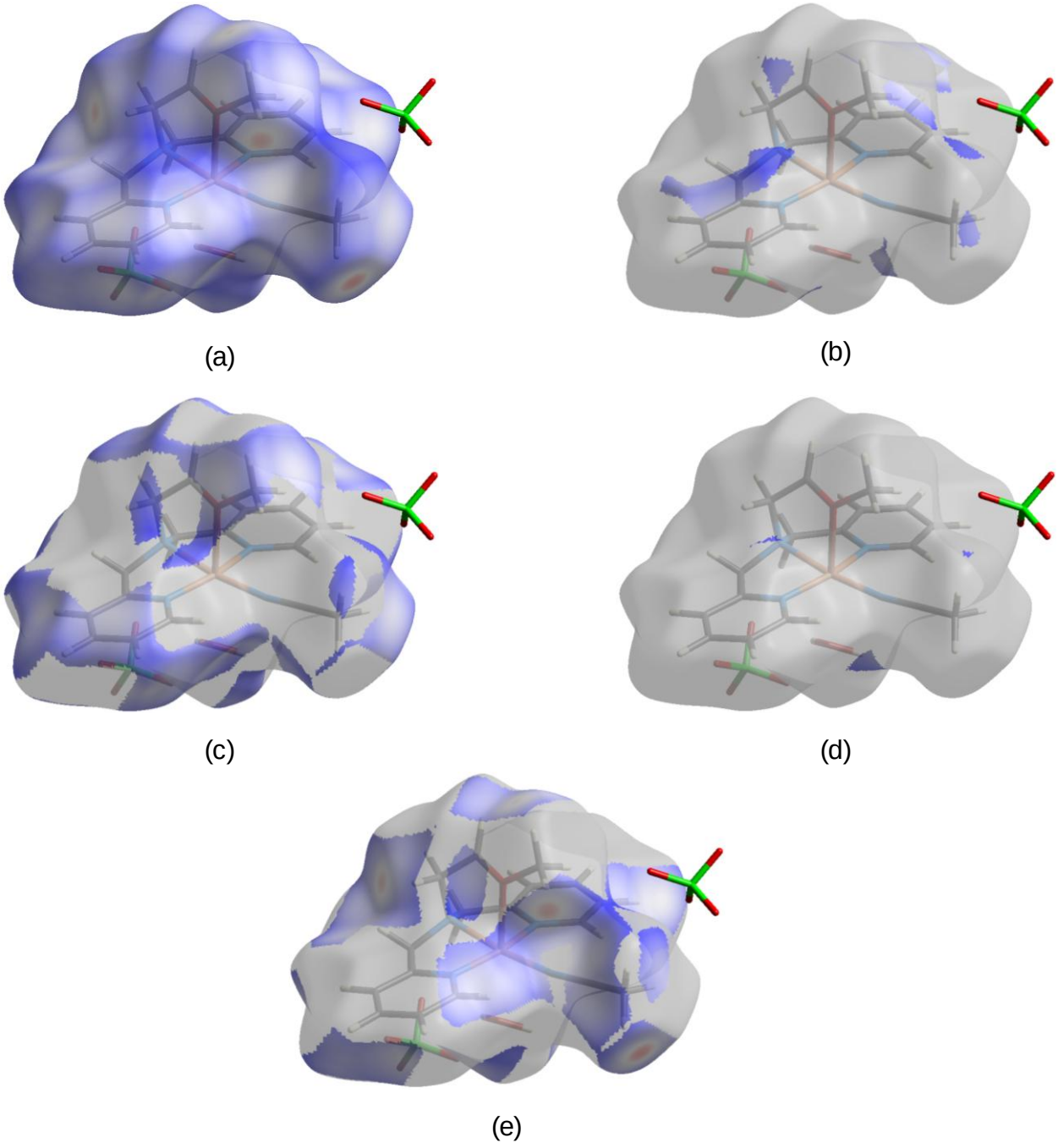

Fig. S34. The Hirshfeld surfaces (**2**) mapped over d_{norm} in the range -0.436 to +0.527 (arbitrary units) for visualizing the weak intermolecular (a) All (b) C···H (c) H···H (d) N···H (d) O···H.

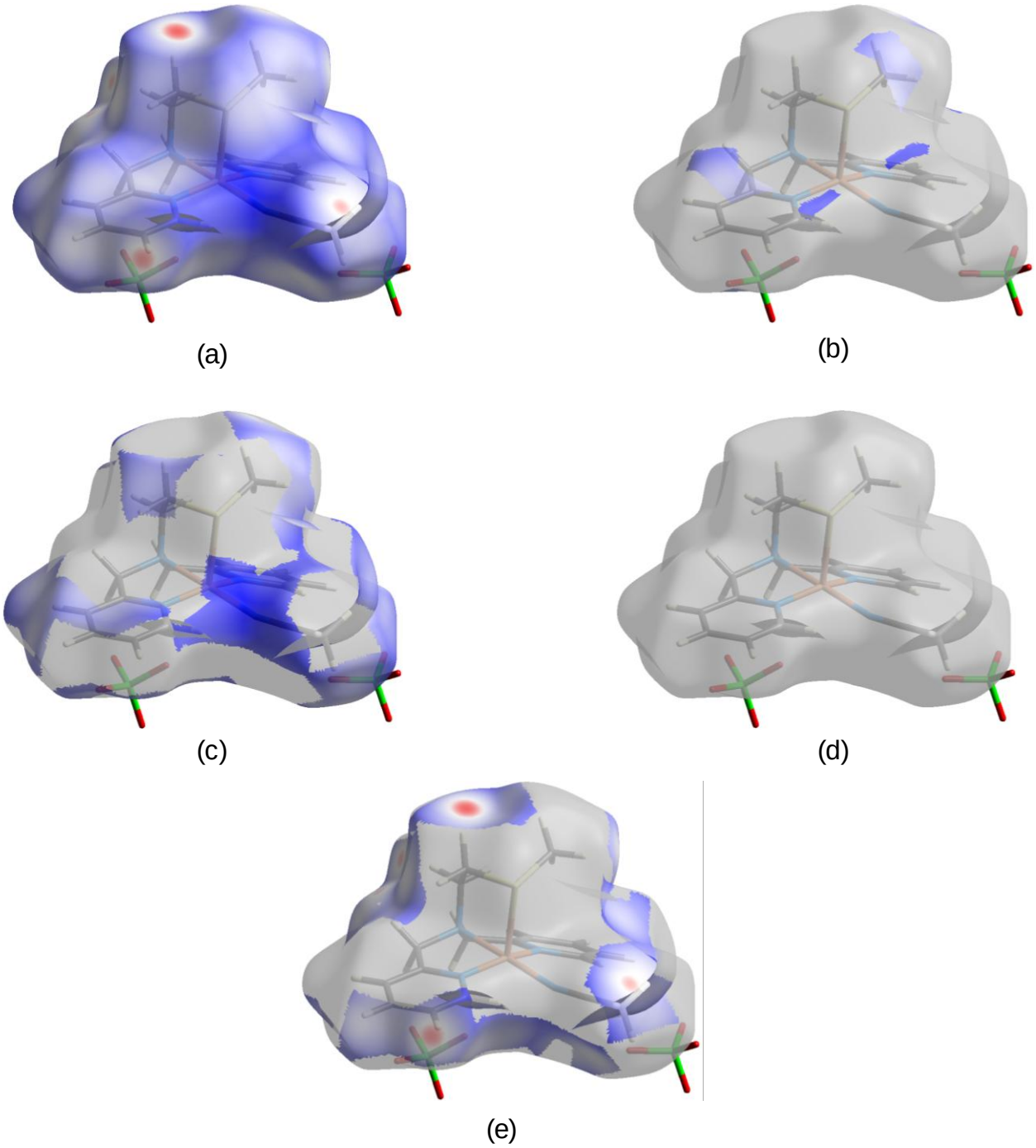

Fig. S35. The Hirshfeld surfaces (**3**) mapped over d_{norm} in the range -0.247 to +0.496 (arbitrary units) for visualizing the weak intermolecular (a) All (b) C···H (c) H···H (d) N···H (d) O···H.

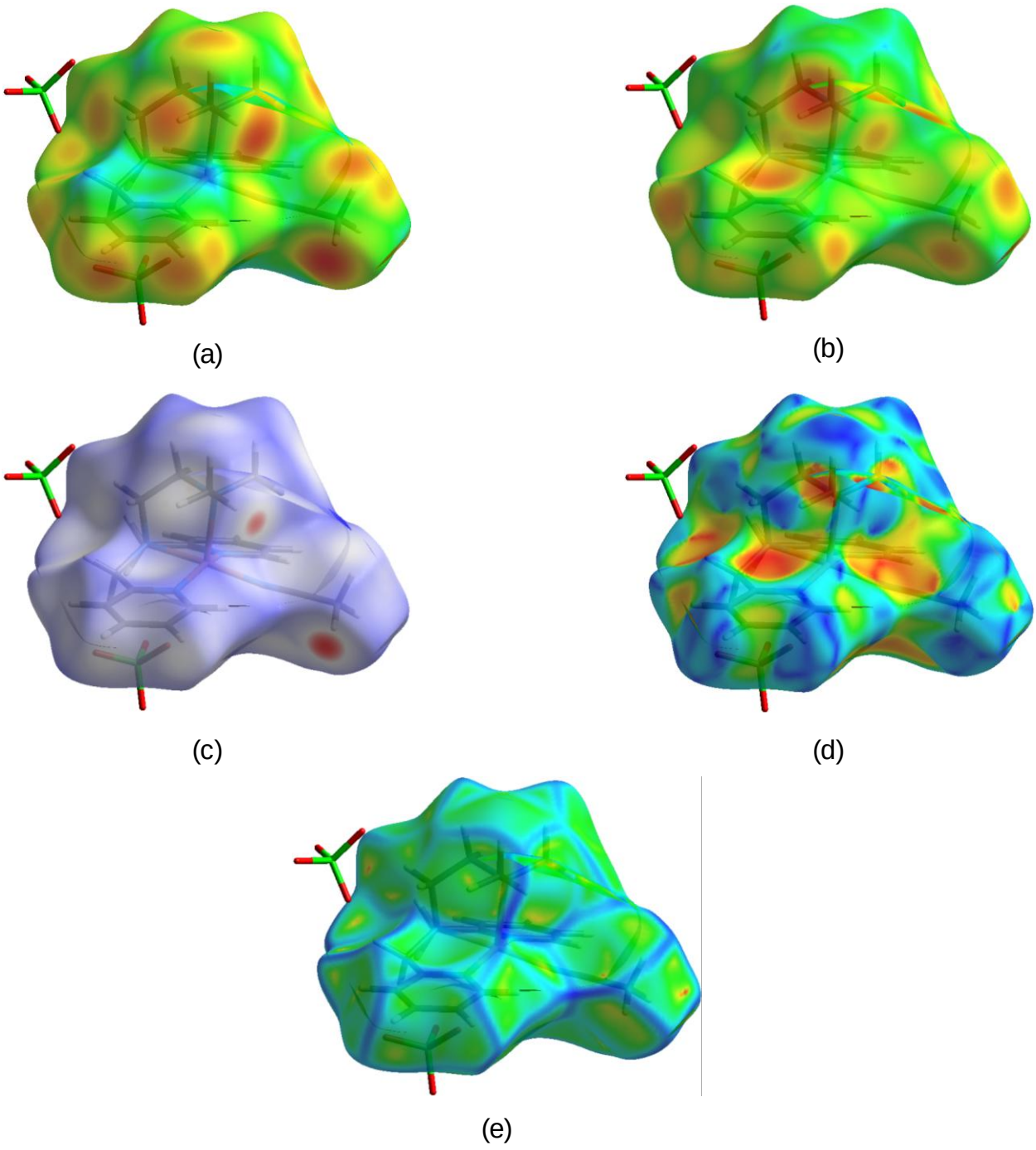

Fig. S36. The Hirshfeld surfaces of complex **1** mapped over d_i, d_e, d_{norm}, shape index and curvedness.

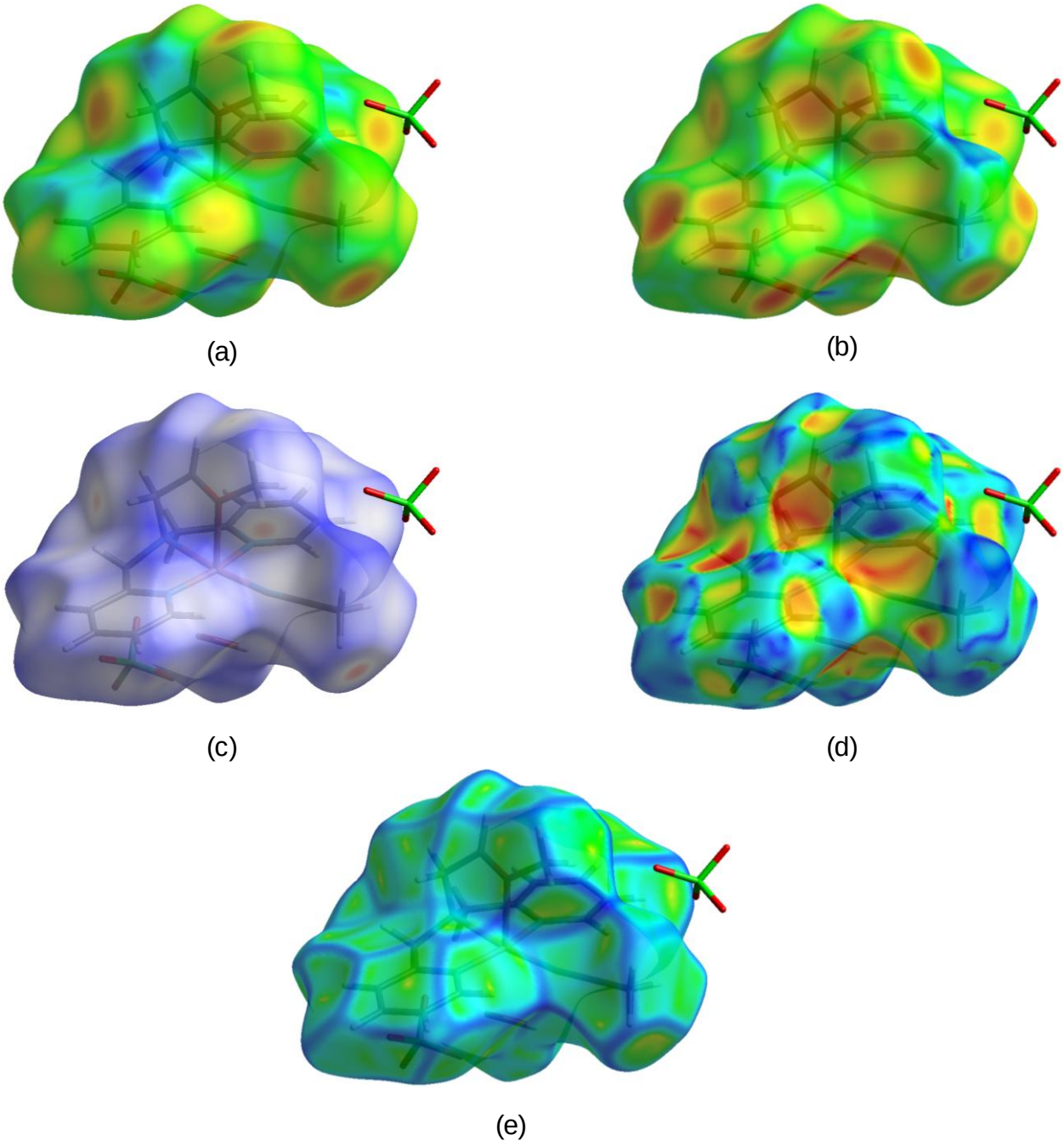

Fig. S37. The Hirshfeld surfaces of complex **2** mapped over d_i, d_e, d_{norm}, shape index and curvedness.

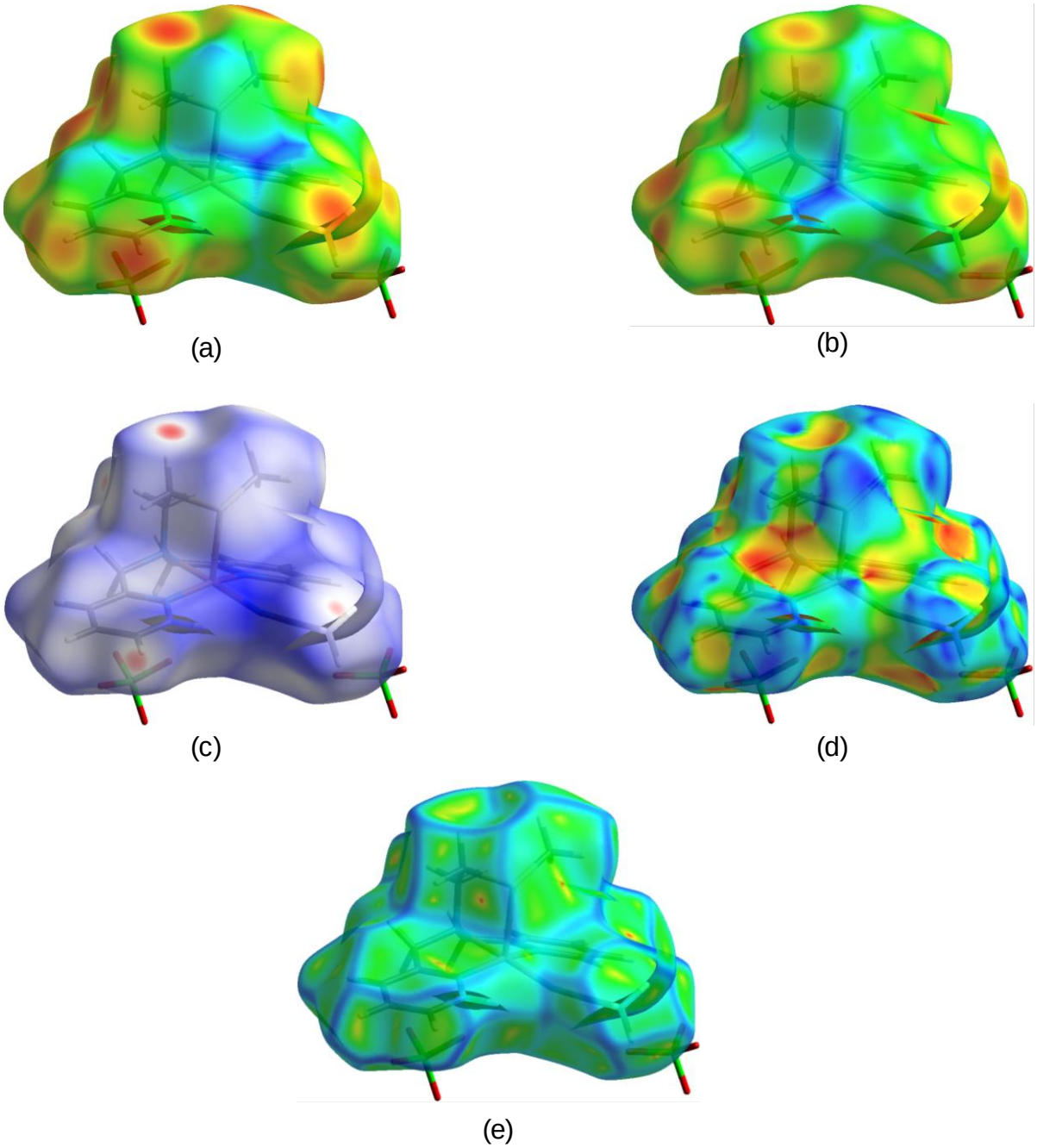

Fig. S38. The Hirshfeld surfaces of complex **3** mapped over d_i, d_e, d_{norm}, shape index and curvedness.

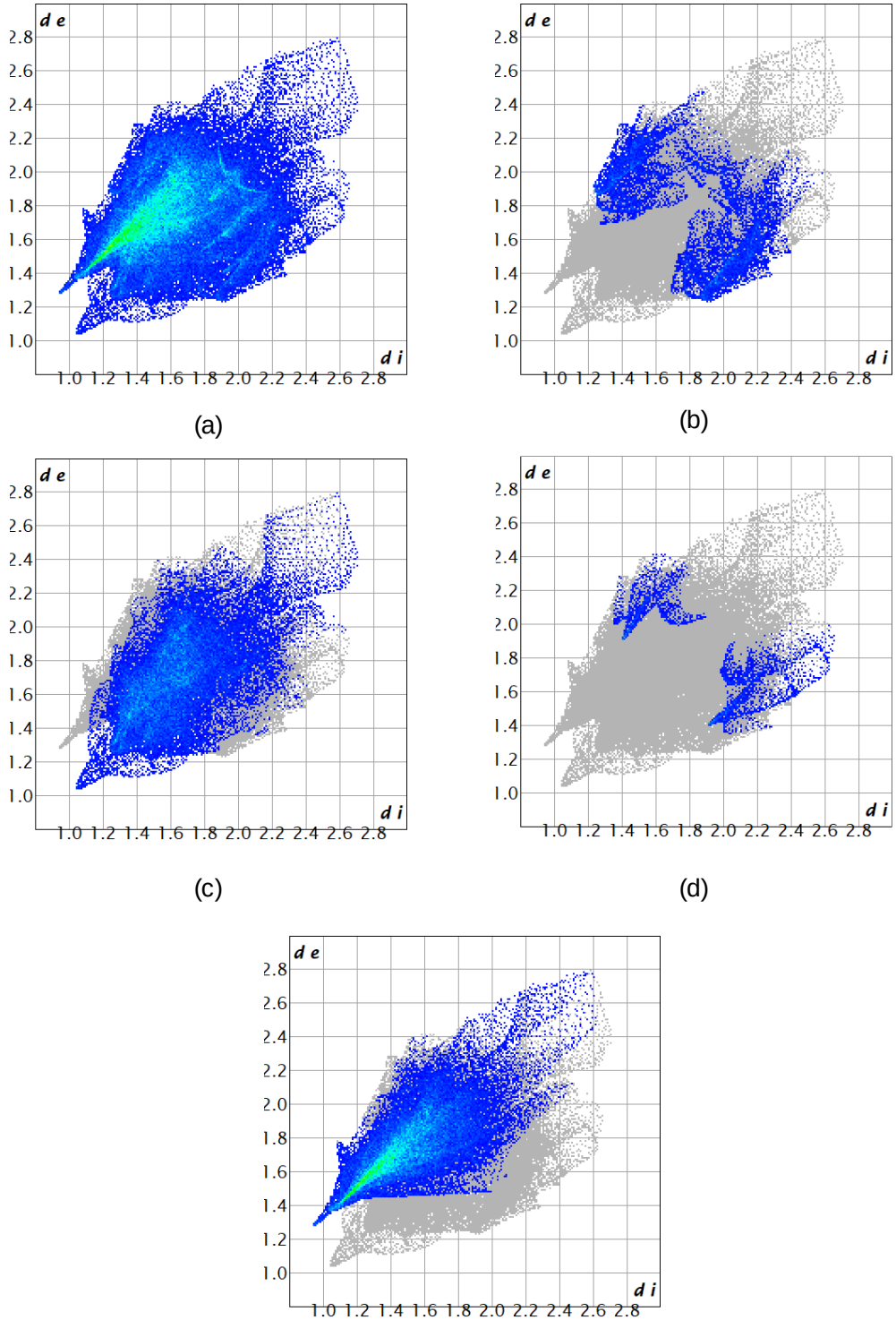

Fig. S39. Hirshfeld surface fingerprint plots for the (a) All (b) C···H (c) H···H (d) N···H (d) O···H contacts of the complex **1**.

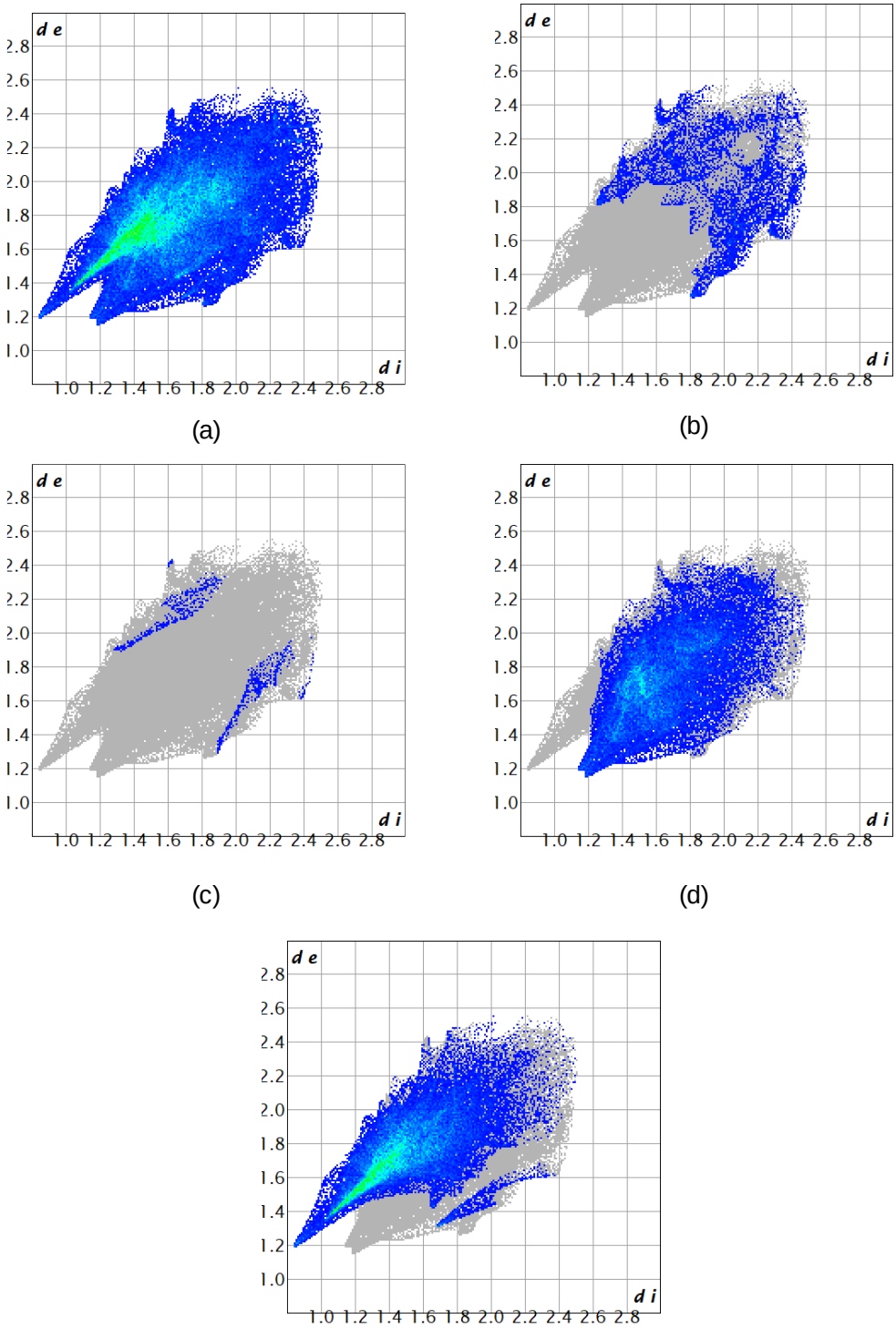

Fig. S40. Hirshfeld surface fingerprint plots for the (a) All (b) C···H (c) H···H (d) N···H (d) O···H contacts of the complex **2**.

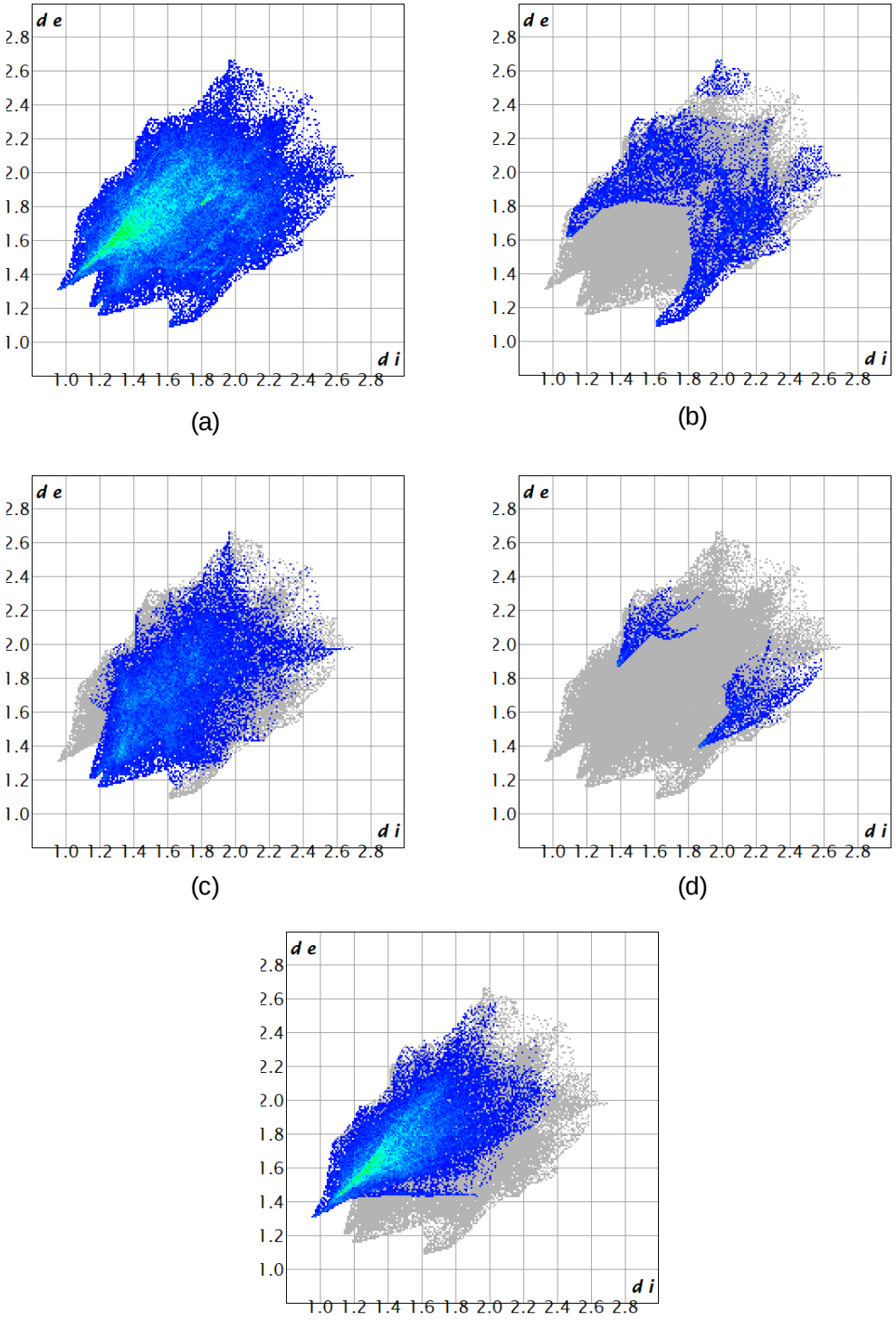

Fig. S41. Hirshfeld surface fingerprint plots for the (a) All (b) C···H (c) H···H (d) N···H (d) O···H contacts of the complex **3**.

Cartesian Coordinates

1

Cu	0.018464507	0.308347010	-0.112256135
N	2.029009313	0.065671641	-0.420402248
N	0.039031375	-1.775103169	-0.383059198
N	-0.177763294	-0.171260591	2.151371196
N	-1.969436740	0.088660599	-0.531770969
N	0.058699755	2.385094674	-0.284652892
C	2.367922740	-1.150264670	-0.908493517
C	3.697266732	-1.503265504	-1.125435043
H	3.942667638	-2.487548824	-1.510642372
C	4.699526055	-0.573443101	-0.844534313
H	5.742060259	-0.826246366	-1.009501987
C	4.343446738	0.679487591	-0.343224032
H	5.092494980	1.427175959	-0.107834748
C	2.997037615	0.959335560	-0.140416233
H	2.671032536	1.913991850	0.255807387
C	1.213952739	-2.061113327	-1.256286766
H	0.920706076	-1.873041309	-2.294646243
H	1.506434746	-3.115988765	-1.186346721
C	0.243327424	-2.341064967	0.993539276
H	-0.028150740	-3.403736996	0.989349144
H	1.311370799	-2.282007210	1.212339299
C	-0.555787906	-1.602111411	2.066935854
H	-0.403210293	-2.115342263	3.027685619
H	-1.625379626	-1.661842028	1.845541444
C	1.094531616	0.000759101	2.892001990
H	1.905290064	-0.546059660	2.408034735
H	1.004601081	-0.350510067	3.929002784
H	1.361466549	1.059849646	2.909355189
C	-1.237242512	0.595949088	2.847433031
H	-0.954798940	1.650516730	2.884388844
H	-1.384078854	0.242058870	3.876815583
H	-2.182136154	0.503100941	2.308467046
C	-1.251836263	-2.200272270	-0.999109602
H	-1.567198476	-3.167295950	-0.591384823
H	-1.090167317	-2.353845302	-2.071227762
C	-2.349200390	-1.172569824	-0.831981610
C	-3.688136435	-1.498783727	-1.044929208
H	-3.966901136	-2.521005807	-1.280185008
C	-4.653423599	-0.497115447	-0.959307498
H	-5.700456238	-0.729971080	-1.125113309
C	-4.254119586	0.806394609	-0.655639012
H	-4.973107110	1.614224834	-0.578861722
C	-2.905070298	1.057009991	-0.443978109

H	-2.546606703	2.048259951	-0.194032216
C	0.100346862	3.526238619	-0.481767232
C	0.150866107	4.959578297	-0.728548588
H	1.103648895	5.220935114	-1.198975160
H	0.054051574	5.503656172	0.215919953
H	-0.666332922	5.248674549	-1.396484620

2

Cu	0.072458684	0.306549503	-0.217160012
O	-0.277765078	0.032340026	2.174454257
N	-1.944554841	0.026265074	-0.413660374
N	0.088783288	2.395037988	-0.218826178
N	2.093061414	0.021269616	-0.165345209
N	0.083027085	-1.778287239	-0.057014920
C	0.120019834	3.552931431	-0.244658096
C	-2.903472214	0.967683384	-0.324773063
H	-2.562360109	1.989192212	-0.202321058
C	1.319044234	-2.192375384	-0.782092705
H	1.578626006	-3.234018877	-0.558489620
H	1.117894045	-2.114191134	-1.854069808
C	2.453182656	-1.257822396	-0.426041585
C	-2.298615475	-1.271312298	-0.553051604
C	3.039467491	0.927291904	0.139452893
H	2.692641235	1.930890231	0.356424792
C	-0.678211496	-1.323910152	2.323276087
H	-1.752914788	-1.436549493	2.120475209
C	-1.164318892	-2.260133684	-0.712074067
H	-0.958557135	-2.375894610	-1.780820198
H	-1.449979778	-3.246859115	-0.329301753
C	-0.887902410	0.909812968	3.128762940
H	-0.503413404	1.910848362	2.931408000
H	-1.980494184	0.906199375	3.026385563
H	-0.619276137	0.615019319	4.149131328
C	-4.256658383	0.656226637	-0.385040293
H	-4.997690060	1.444531391	-0.314600552
C	3.786407618	-1.657155942	-0.396885991
H	4.049222272	-2.689736084	-0.601967892
C	0.160065262	5.007966381	-0.276229517
H	-0.739915950	5.394006942	-0.764326600
H	0.211530189	5.400571809	0.743806260
H	1.039344652	5.342818938	-0.834835447
C	-3.636516491	-1.657953936	-0.611229954
H	-3.894921351	-2.706469102	-0.718428676
C	-4.629250380	-0.681279332	-0.531052293
H	-5.677014109	-0.960945566	-0.576107095

C	0.178582965	-2.165600878	1.390028362
H	-0.081831030	-3.226220577	1.496722259
H	1.222014003	-2.043163339	1.687303408
C	4.770419788	-0.713178423	-0.096744716
H	5.815947268	-1.003150405	-0.068534783
C	4.390835534	0.600675969	0.179183160
H	5.123717115	1.359979455	0.427733909
O	0.214045263	0.140412813	-2.669081677
H	-0.539241851	0.376793118	-3.227662215
H	0.992252333	0.462566769	-3.144569719
H	-0.497818991	-1.669373427	3.350253792

3

Cu	0.003781271	0.418536357	-0.104127900
S	0.350952775	-0.540813719	2.360583374
N	-1.986729115	0.181246716	-0.372685864
N	0.026195385	-1.585612035	-0.797894779
N	2.006657141	0.246306478	-0.344514347
C	2.412547548	-0.888800996	-0.957651829
N	-0.044494018	2.505304721	-0.084017148
C	1.323858340	-1.786024249	-1.505887397
C	-2.318402682	-0.895499914	-1.123446956
C	-1.156956598	-1.671173529	-1.703914065
C	-0.151730879	-2.508357878	0.369581674
C	-0.068757386	3.661165524	-0.160632814
C	4.287528504	0.891485311	-0.007264744
C	2.923190861	1.114796115	0.127807588
C	-3.648453750	-1.219821627	-1.376002662
C	-2.956709012	0.959983781	0.143467598
C	3.765331854	-1.179101792	-1.119899151
C	-0.097707229	5.112910347	-0.253487916
C	4.715528825	-0.275107556	-0.643725465
C	0.697848280	-2.177973862	1.599609059
C	-4.655539461	-0.408035600	-0.850476635
C	-4.304509839	0.699243884	-0.076497378
C	-1.208065229	-0.865581375	3.263711669
H	-2.630403477	1.804143680	0.740645072
H	-5.057984977	1.349707527	0.353314254
H	-5.698825737	-0.641157309	-1.038349333
H	-3.891442635	-2.090694918	-1.975979678
H	2.538014574	1.996615013	0.626397878
H	4.994661822	1.613707918	0.384773545
H	5.774337373	-0.482630400	-0.761652419
H	4.068880497	-2.097325270	-1.612341418
H	1.630337577	-2.837615317	-1.463028951

H	1.178059805	-1.544163851	-2.564185104
H	-0.882605880	-1.228937737	-2.667685659
H	-1.434972121	-2.714994005	-1.893492507
H	-1.209496003	-2.482797309	0.641351036
H	0.074871139	-3.531795276	0.040102805
H	0.750359533	5.461972827	-0.850479768
H	-1.027364211	5.434956529	-0.732371412
H	-0.037715756	5.550103435	0.747884333
H	1.766960110	-2.183306794	1.375473315
H	0.531724814	-2.949755273	2.356553589
H	-1.454439483	0.058025726	3.791075592
H	-2.028465885	-1.129283877	2.594311392
H	-1.044810952	-1.654670756	4.000100086